

Supporting Information for:

High Degree of Silanization of Olive Wood Shell Stone and Their Use in Polyester Biocomposites

Melissa Olmedo-Navarro,^a Juana M. Pérez,*^a Natalia Gutiérrez-Segura,^a Bernardo Sánchez-Sevilla,^a Yolanda Soriano-Jerez,^b Diego A. Alonso,^c Mari Carmen Cerón^{a,b} and Ignacio Fernández*^a

^a Department of Chemistry and Physics. Research Centre CIAIMBITAL. University of Almería. Ctra. Sacramento. s/n. 04120. Almería. Spain. Email: ifernan@ual.es

^b Department of Chemical Engineering, University of Almería, 04120 Almería, Spain

^c Departamento de Química Orgánica, Facultad de Ciencias, and Instituto de Síntesis Orgánica (ISO), Universidad de Alicante, Apdo. 99, 03080 Alicante, Spain

Table of Contents:

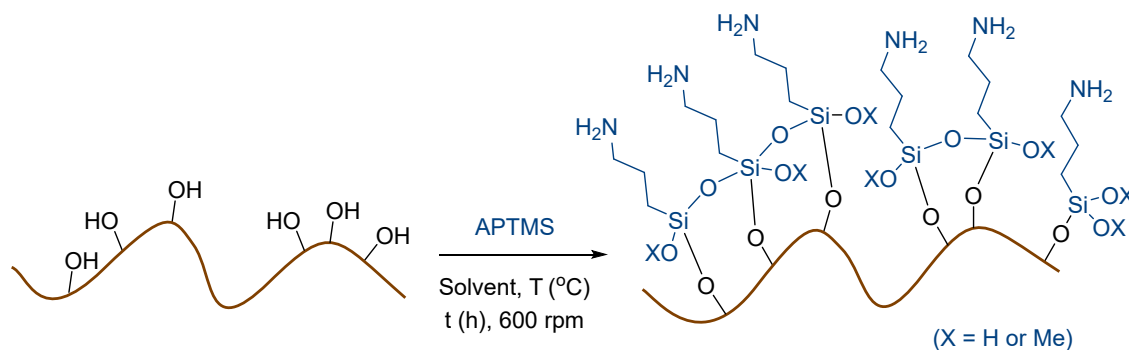
1. Optimization of the reaction conditions for the silanization of OS with different silanes	3
2. FESEM measurements	7
3. Particle size distribution of deposited and suspended functionalized OS materials.	15
4. IR Spectra	19
5. ζ -Potential and Electrophoretic mobility	29
6. Particle size distribution of deposited and suspended OS and OS@Silanized biofillers.....	32
7. Mechanical properties	42
8. Colorimetry	45
9. SEM images	47
10. Static contact angle measurements	50
11. References	52

1. Optimization of the reaction conditions for the silanization of OS with different silanes

The optimization of the reaction conditions for the highly and efficient attachment of silane on the surface of virgin olive good shell stone (OS) by the “grafting to” approach using silanes with different nature such as (3-aminopropyl)trimethoxysilane (APTMS) and γ -methacryloxypropyltrimethoxysilane (MEMO) was carried out.

The study was started with the optimization of the reaction conditions for the 'grafting to' approach using 1g of virgin OS and 114M solution of APTMS (Table S1). Initially, the reaction was performed using the optimal reaction conditions previously reported by the group,¹ where toluene was used as solvent and the reaction was heated at reflux during 2h obtaining 22.4 mg/g of Si, that correspond to the 13.7% (0.79 mmol) of the initial APTMS added to the reaction mixture in the silanization process (entry 1). It should be noted that native OS was also analyzed by XRF measurements observing the presence of traces of Si (0.11 mg/g). After that, the evaluation of the use of different solvents heating at reflux (entries 2-5) was carried out, obtaining the best result with hexane after 2h (entry 5). Furthermore, the use of mixture of different solvent was evaluated without any improvement on the results (entries 6 and 7). The decrease of the temperature gives to the reduction of the silane grafted from 33.6 to 16.9 mg/g of Si (entry 8). When the reaction was carried out at lower or even higher concentrations of APTMS the result previously obtained could not be improved (entries 9-12). Finally, the time of the reaction was tested (entries 13-16) obtaining a considerable increase after 24h and 72h reaching values of 40.98 and 42.55 mg/g of Si.

Table S1. Optimization of the reaction conditions for the silanization using APTMS.^a

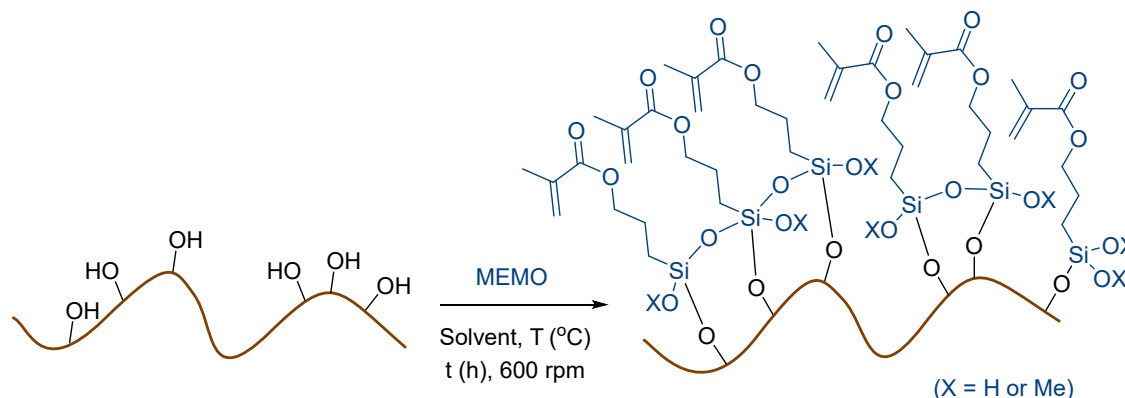


Entry	[APTMS] (mM)	Solvent (mL)	T (°C)	t (h)	[Si] ^{b,c} (mg/g)
1	114	PhMe	110	2	22.4 (13.7)
2	114	Acetone	60	2	1.6 (1.0)
3	114	H ₂ O	110	2	17.2 (10.9)
4	114	EtOH	85	2	3.3 (2.1)
5	114	Hexane	75	2	33.6 (21.2)
6	114	PhMe/EtOH (1:1)	110	2	2.4 (1.5)
7	114	PhMe/H ₂ O (1:1)	110	2	19.0 (12.0)
8	114	Hexane	25	2	16.9 (10.1)
9	28	Hexane	75	2	4.6 (11.8)
10	56	Hexane	75	2	26.2 (33.2)
11	85	Hexane	75	2	32.4 (26.7)
12	171	Hexane	75	2	20.2 (8.4)
13	114	Hexane	75	5	34.1 (29.0)
14	114	Hexane	75	16	37.1 (31.3)
15	114	Hexane	75	24	41.0 (34.6)
16	114	Hexane	75	72	42.5 (35.2)

^a Reaction carried out using 1g of virgin OS, 5.8 mmol of APTMS in 50 mL of the corresponding solvent and stirring the reaction at 600 rpm. ^b Data determined using XRF analysis. ^c In brackets the percentage of initially added APTMS incorporated on the OS.

The optimization of the reaction conditions using γ -methacryloxypropyltrimethoxysilane (MEMO) were also studied. Initially, different solvents and mixtures of them were tested (entries 1-7) obtaining promising results when the greenest solvent (H_2O) were used (entry 3), fact that positively affect the sustainability of the process. In view of the good results obtained in aqueous medium, an exhaustive analysis of the pH of the reaction mixture was also carried out (entries 8-13), being able to increase the degree of functionalization of the OS more than 4.5 times (from 2.9 mg/g to 13.6 mg/g of Si when pH was decrease until 1.5 using acetic acid (entry 8). Variation on the temperature of the reaction (entry 14) or the concentration of silane (entries 15-17) did not positively influence on the results obtained. Finally, the time of the reaction (entries 18-22) was increased using the reaction conditions of entry 8, obtaining high efficiency on the anchoring process with the increase of the time as it was previously observed with APTMS (**Table S1**).

Table S2. Optimization of the reaction conditions for the silanization using MEMO.^a

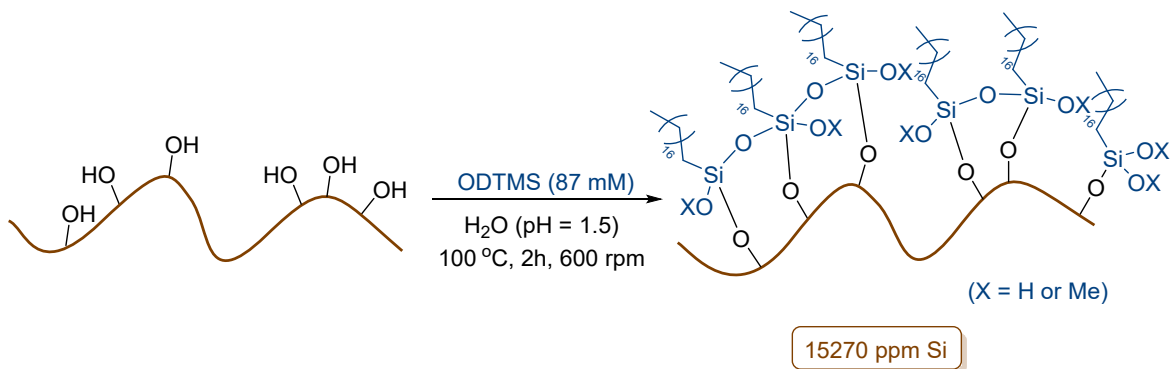


Entry	[MEMO] (mM)	Solvent (mL)	T (°C)	t (h)	[Si] ^{b,c} (mg/g)
1	87	PhMe	110	2	0.26 (0.22)
2	87	Acetone	60	2	0.25 (0.21)
3	87	H_2O (pH 5.8)	110	2	2.93 (2.34)
4	87	EtOH	85	2	0.14 (0.12)
5	87	Hexane	75	2	0.34 (0.28)
6	87	PhMe/EtOH (1:1)	110	2	0.18 (0.15)
7	87	PhMe/ H_2O (1:1)	110	2	0.29 (0.24)
8	87	H_2O (pH 1.5) ^b	100	2	13.6 (10.72)

9	87	H ₂ O (pH 2.5) ^b	100	2	2.14 (1.77)
10	87	H ₂ O (pH 3.5) ^b	100	2	0.15 (0.12)
11	87	H ₂ O (pH 4.5) ^b	100	2	0.20 (0.16)
12	87	H ₂ O (pH 7.0) ^b	100	2	1.59 (1.31)
13	87	H ₂ O (pH 8.0) ^b	100	2	0.59 (0.51)
14	87	H ₂ O (pH 5.8)	25	2	0.21 (0.17)
15	21	H ₂ O (pH 1.5) ^b	100	2	0.34 (1.13)
16	41	H ₂ O (pH 1.5) ^b	100	2	1.91 (3.25)
17	61	H ₂ O (pH 1.5) ^b	100	2	8.70 (9.86)
18	87	H ₂ O (pH 1.5) ^b	100	5	12.24 (10.06)
19	87	H ₂ O (pH 1.5) ^b	100	16	16.86 (14.28)
20	87	H ₂ O (pH 1.5) ^b	100	24	36.90 (31.03)
21	87	H ₂ O (pH 1.5) ^b	100	48	40.86 (34.27)
22	87	H ₂ O (pH 1.5) ^b	100	72	44.08 (37.13)

^a Reaction carried out using 1g of virgin OS, 4.2 mmol of MEMO in 50 mL of the corresponding solvent and stirring the reaction at 600 rpm. ^bpH of the reaction adjusted using acetic acid or sodium acetate aqueous solution. ^c Data determined using XRF analysis. ^d In brackets the percentage of initially added MEMO incorporated on the OS.

With the optimal conditions in hand for MEMO silane, the reaction was tested using a non-functionalized silane such as octadecyltrimethoxysilane (ODTMS), obtaining 15.3 mg/g of Si anchored on the surface of the initial virgin OS (**Scheme S1**). This is a promising result that will help to study deeply the interaction of functional groups at the end of the chain in silanes anchored in biodegradable matrix with polymers used for the formation of composites.



Scheme S1. Silanization of virgin OS with ODTMS.

2. FESEM measurements

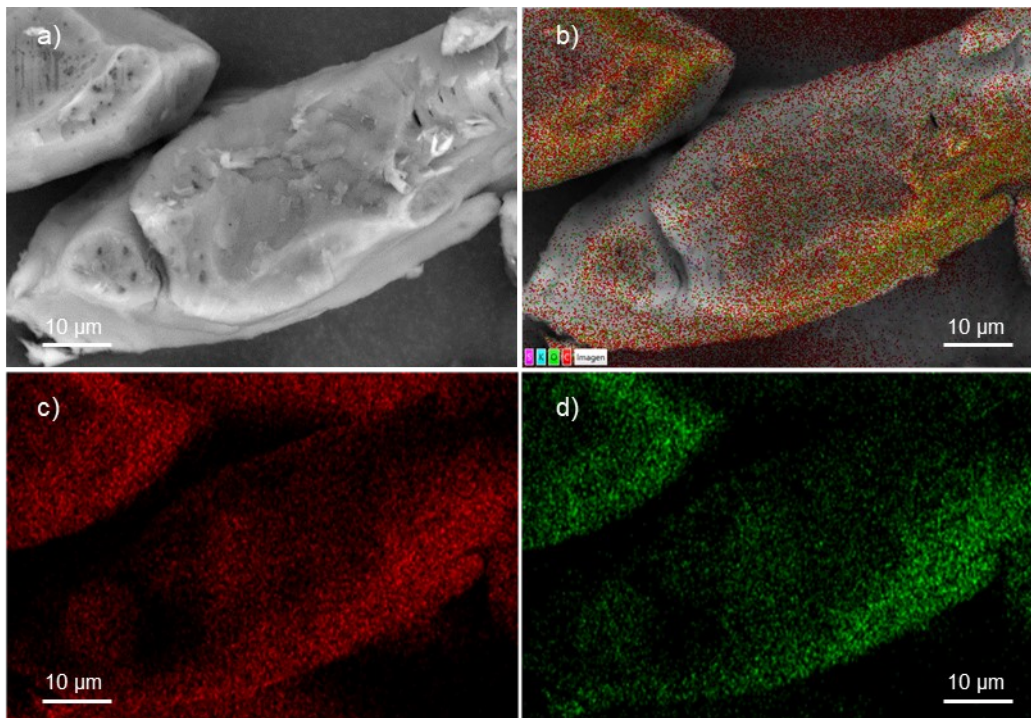


Figure S1. FESEM-EDX micrographs of OS: a) HDBSD; b) Overall mapping; c) carbon; and d) oxygen.

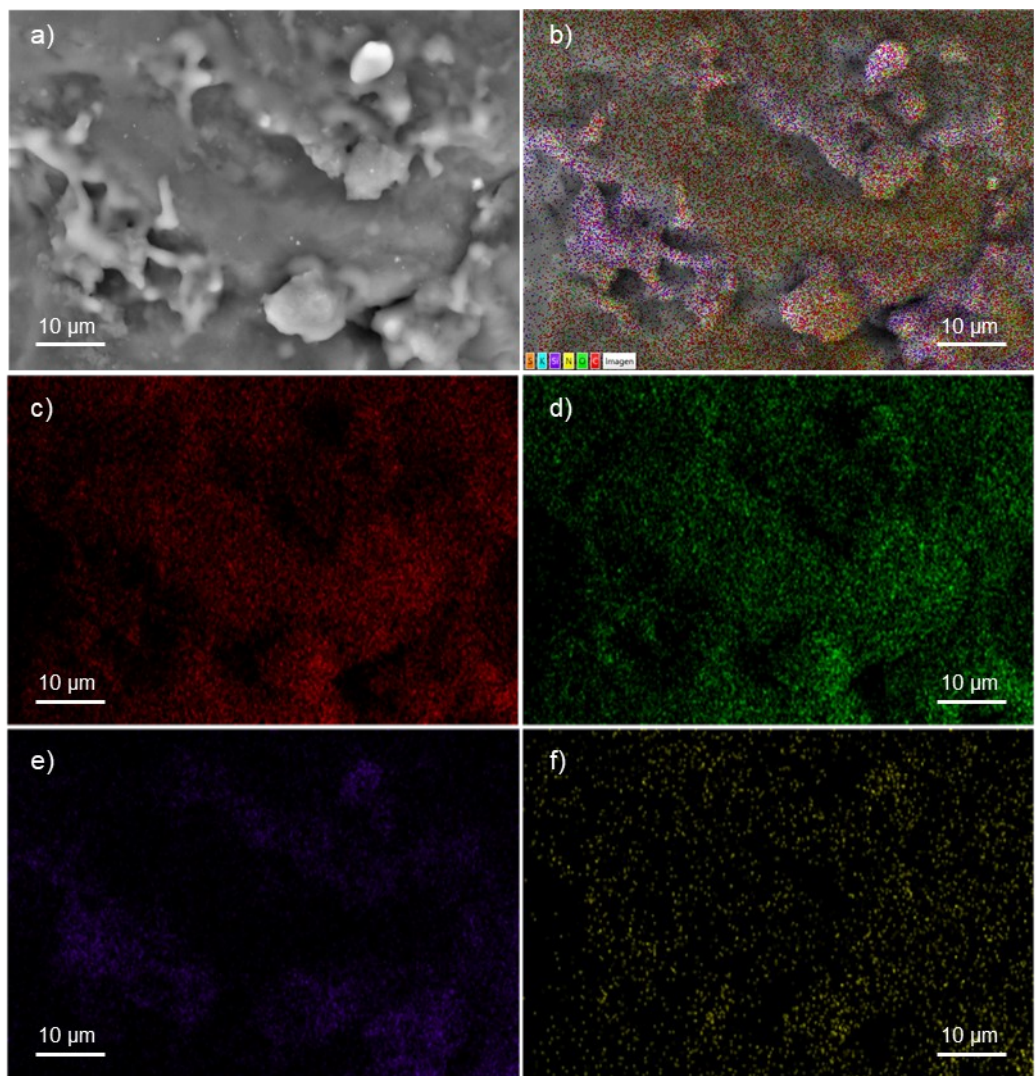


Figure S2. FESEM-EDX micrographs of OS@AEAPTMS: a) HDBSD; b) Overall mapping; c) carbon; d) oxygen; e) silicon; and f) nitrogen.

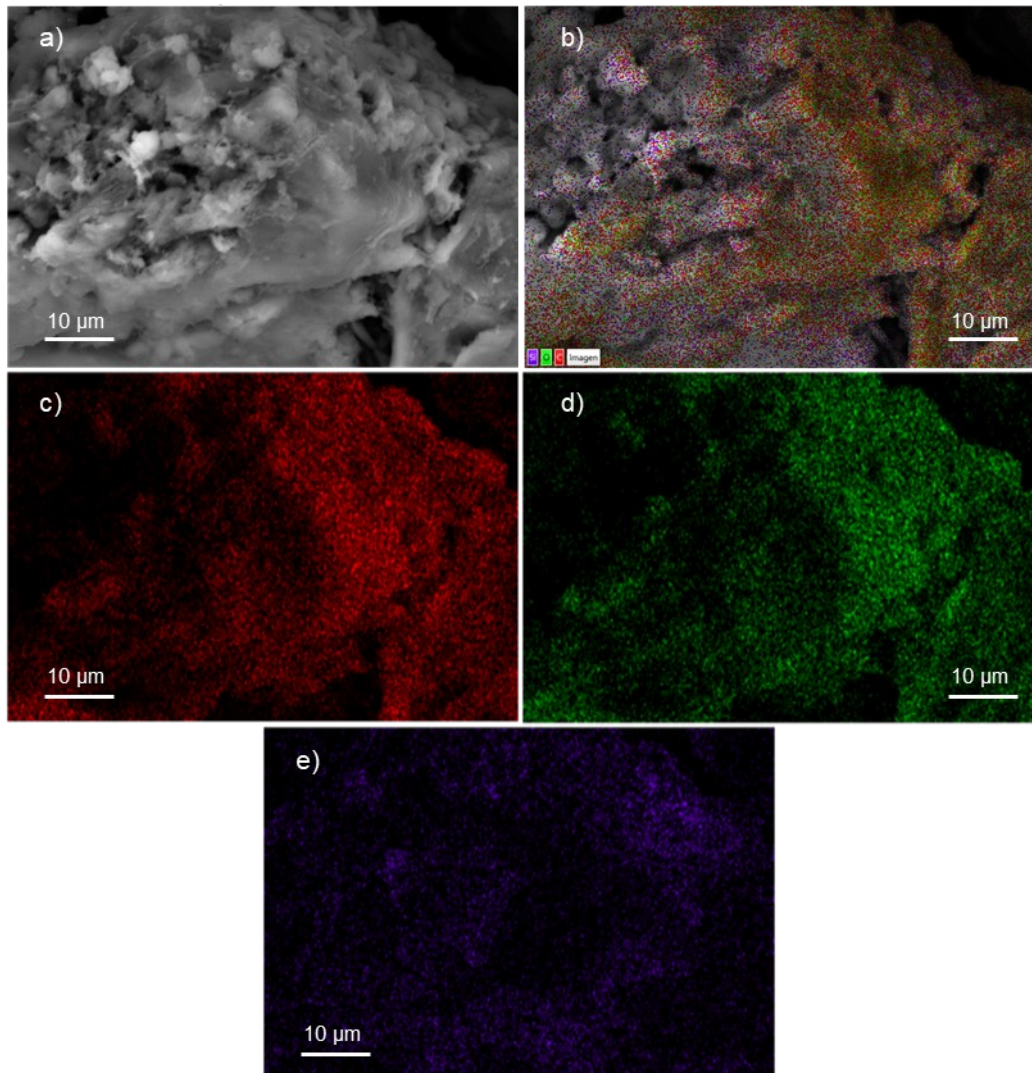


Figure S3. FESEM-EDX micrographs of OS@MEMO: a) HDBSD; b) Overall mapping; c) carbon; d) oxygen; and e) silicon.

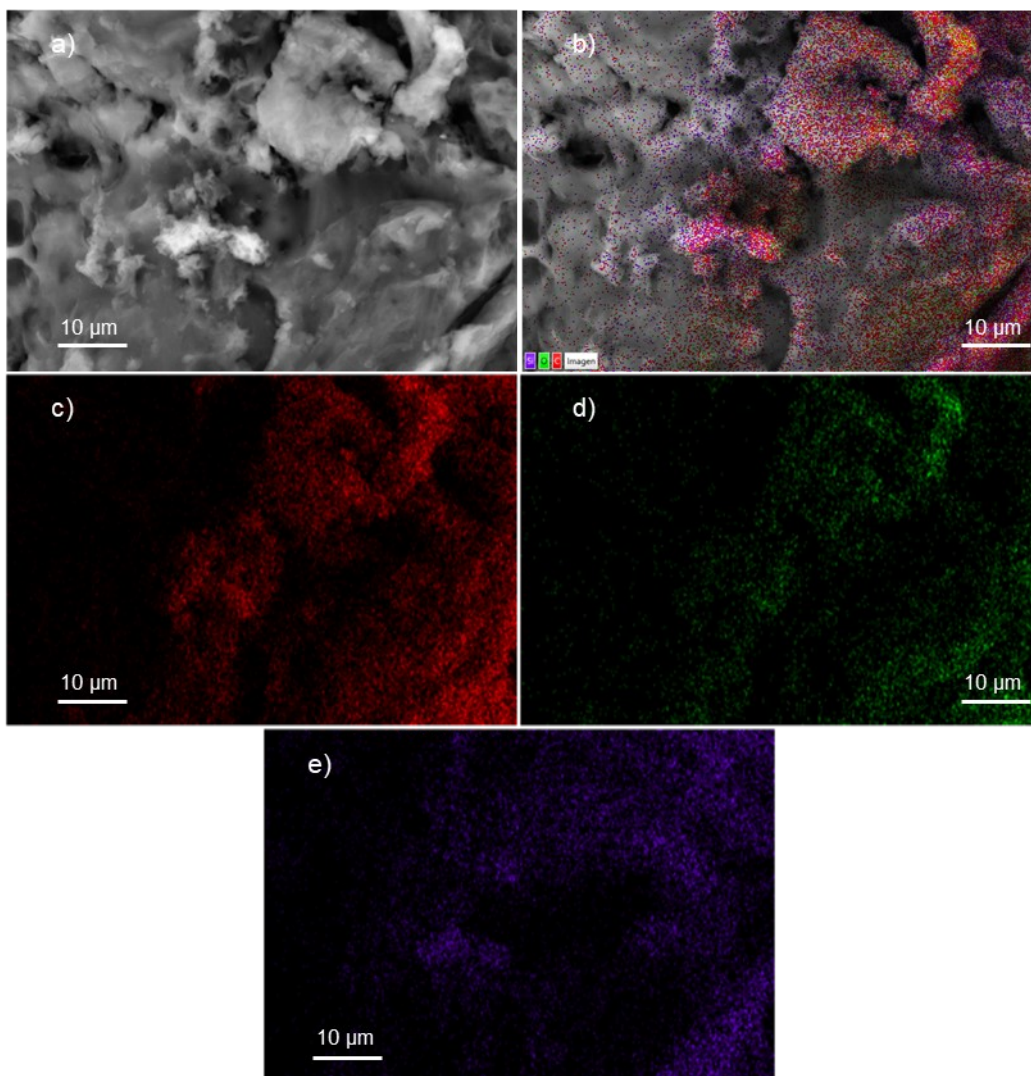


Figure S4. FESEM-EDX micrographs of OS@ODTMS: a) HDBSD; b) Overall mapping; c) carbon; d) oxygen; and e) silicon.

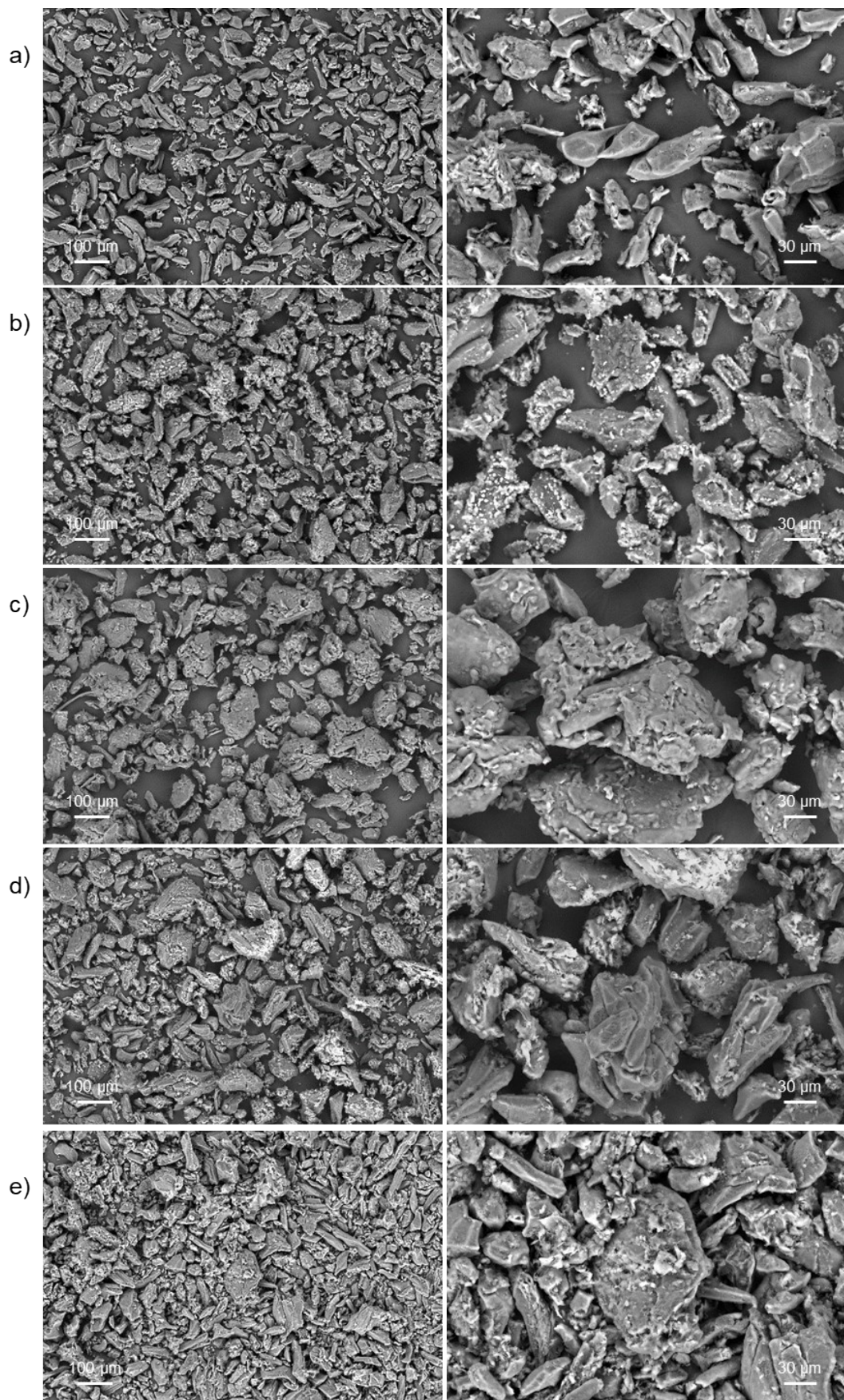


Figure S5. FESEM (HDBSD) images of a) native OS, b) OS@APTMS; c) OS@AEAPTMS; d) OS@MEMO and e) OS@ODTMS.

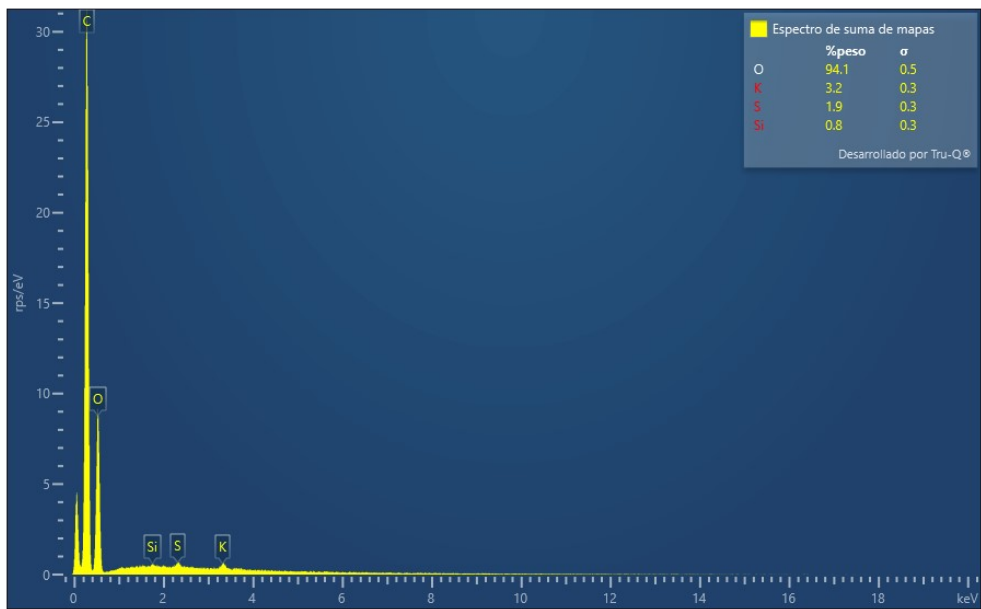


Figure S6. EDX spectrum of initial OS.

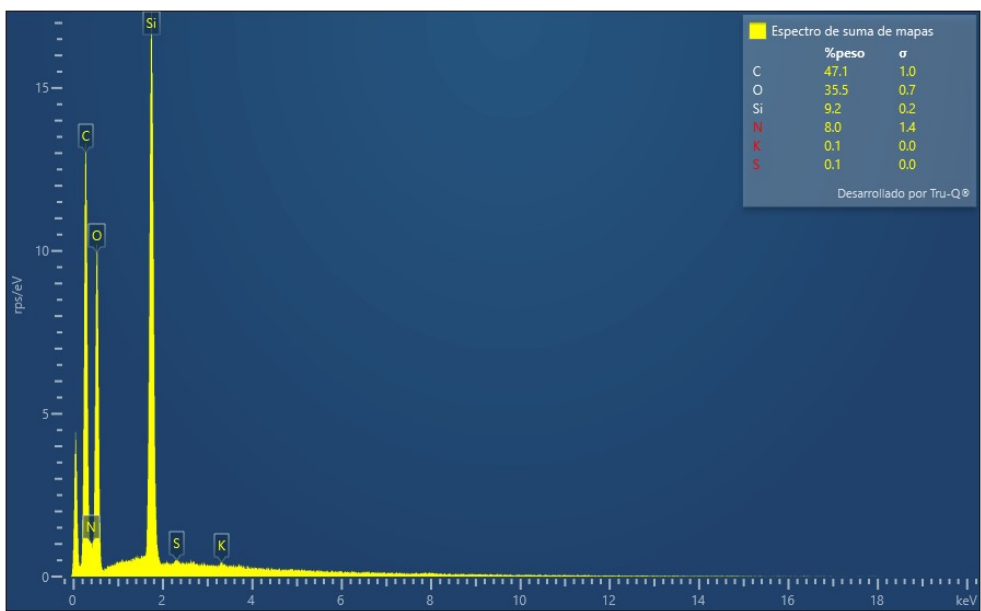


Figure S7. EDX spectrum of OS@APTMS.

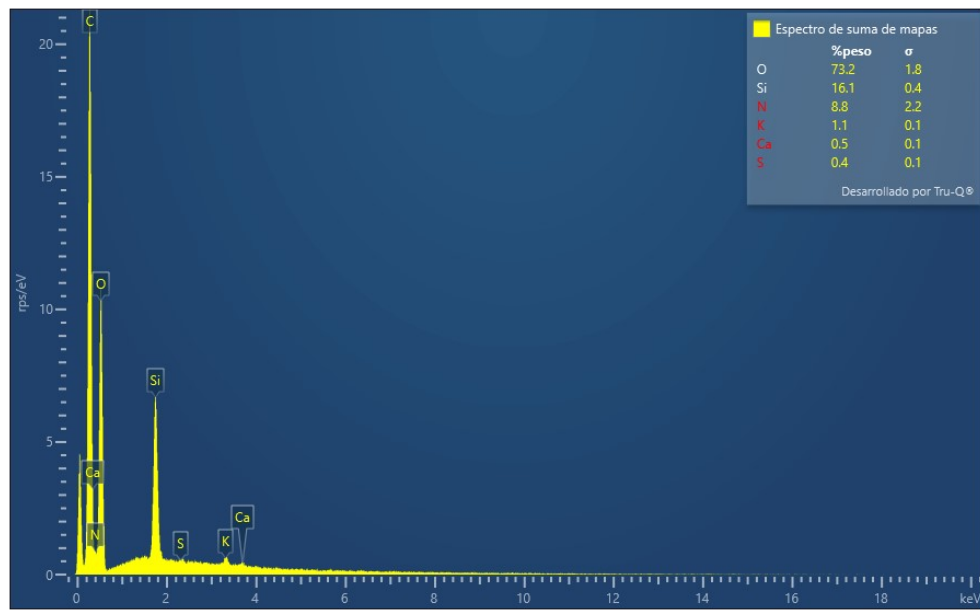


Figure S8. EDX spectrum of OS@AEAPTMS.

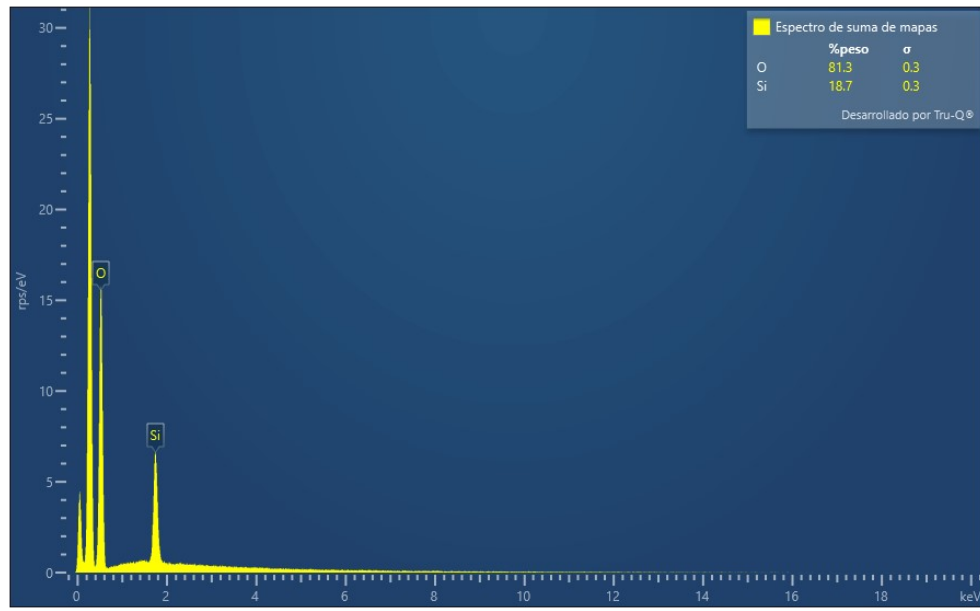


Figure S9. EDX spectrum of OS@MEMO.

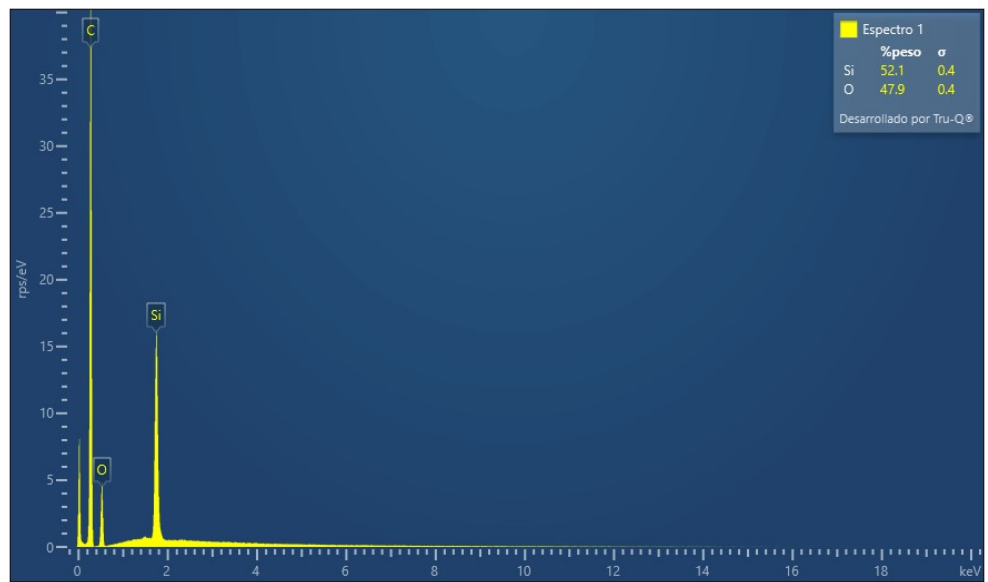


Figure S10. EDX spectrum of OS@ODTMS.

3. Particle size distribution of deposited and suspended functionalized OS materials.

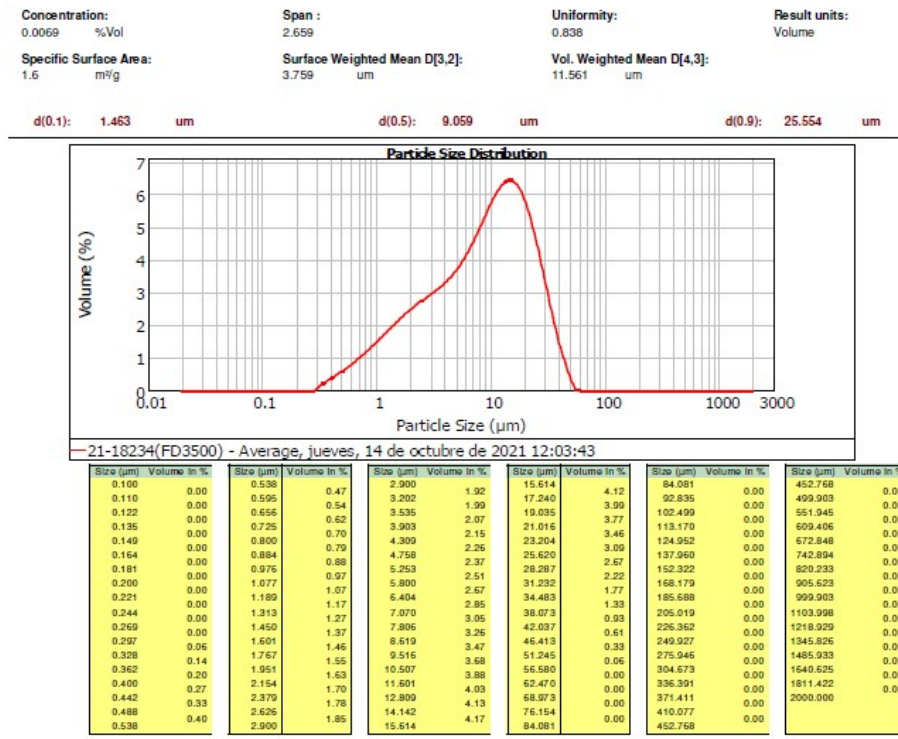


Figure S11. Particle size distribution of sodium feldspar.

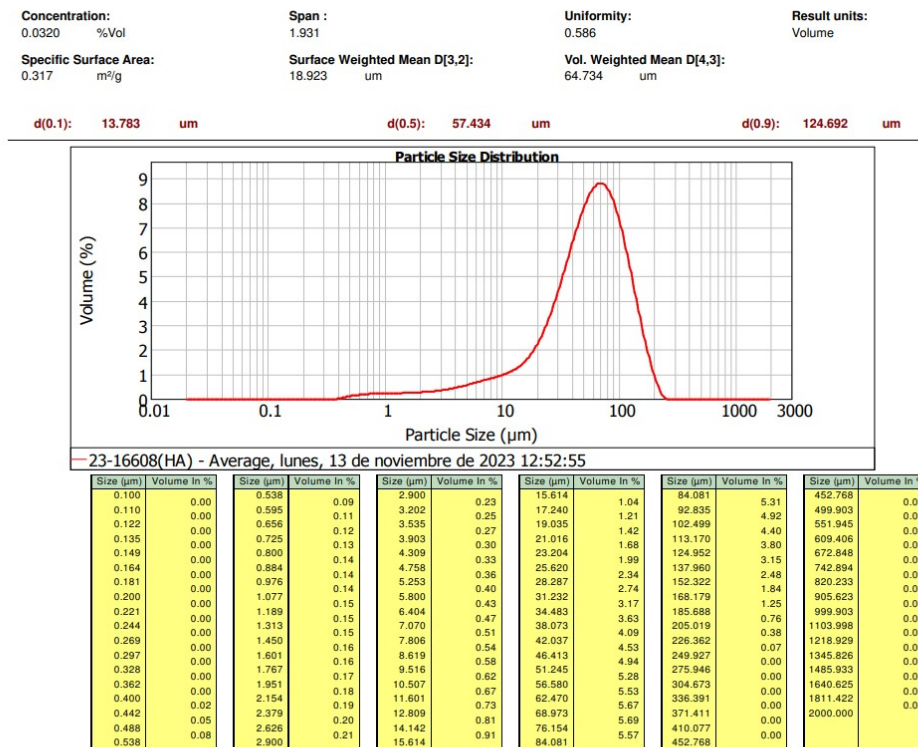


Figure S12. Particle size distribution of initial OS.

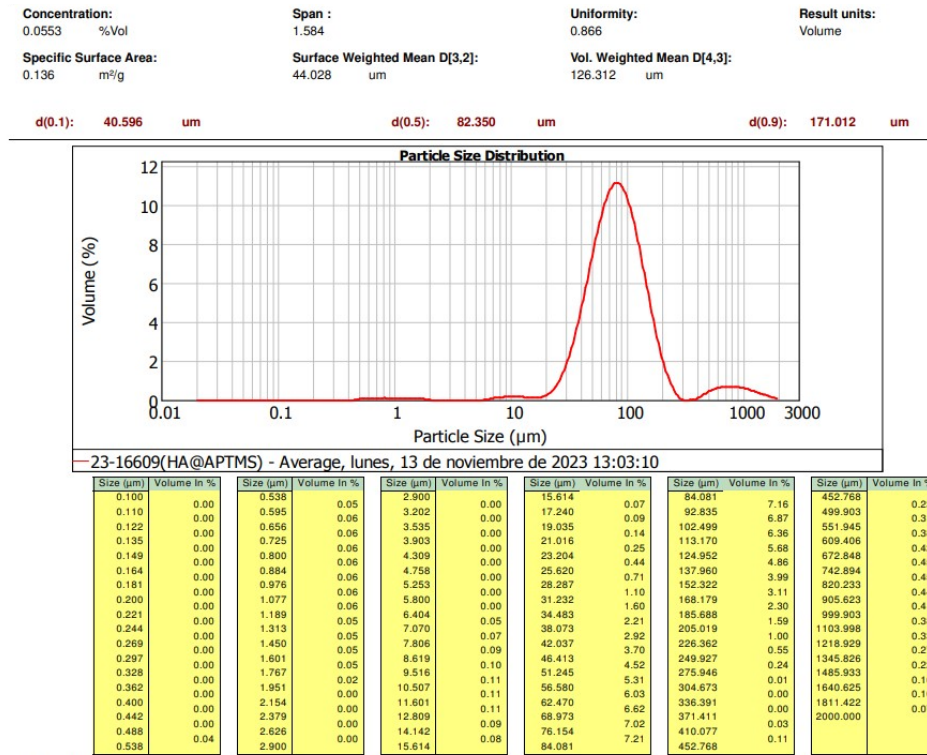


Figure S13. Particle size distribution of OS@APTMS.

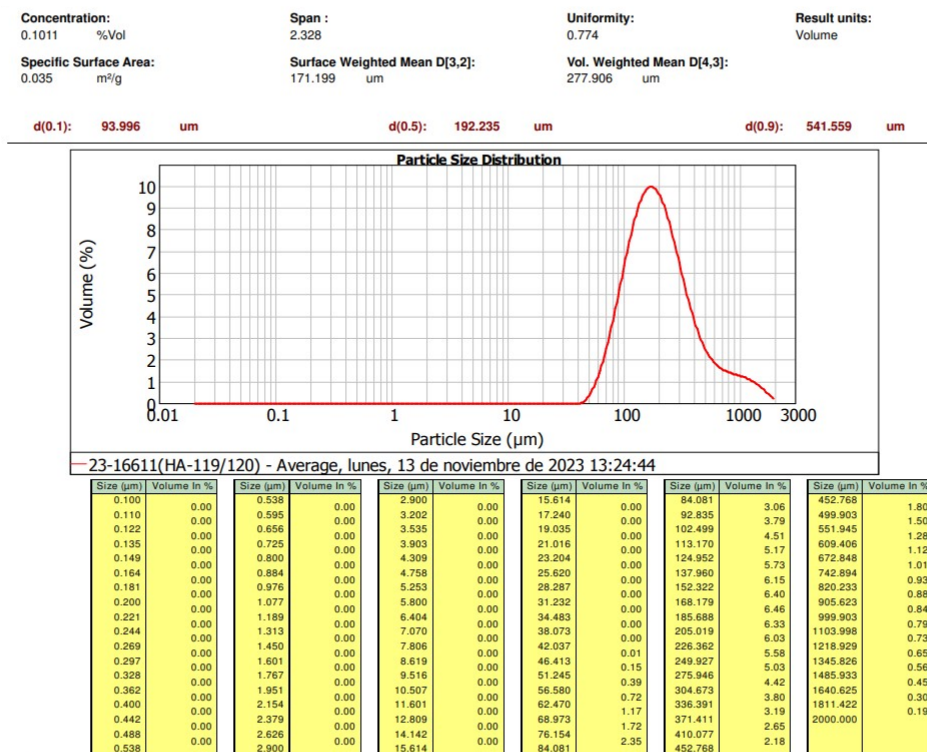


Figure S14. Particle size distribution of OS@AEAPTMS.

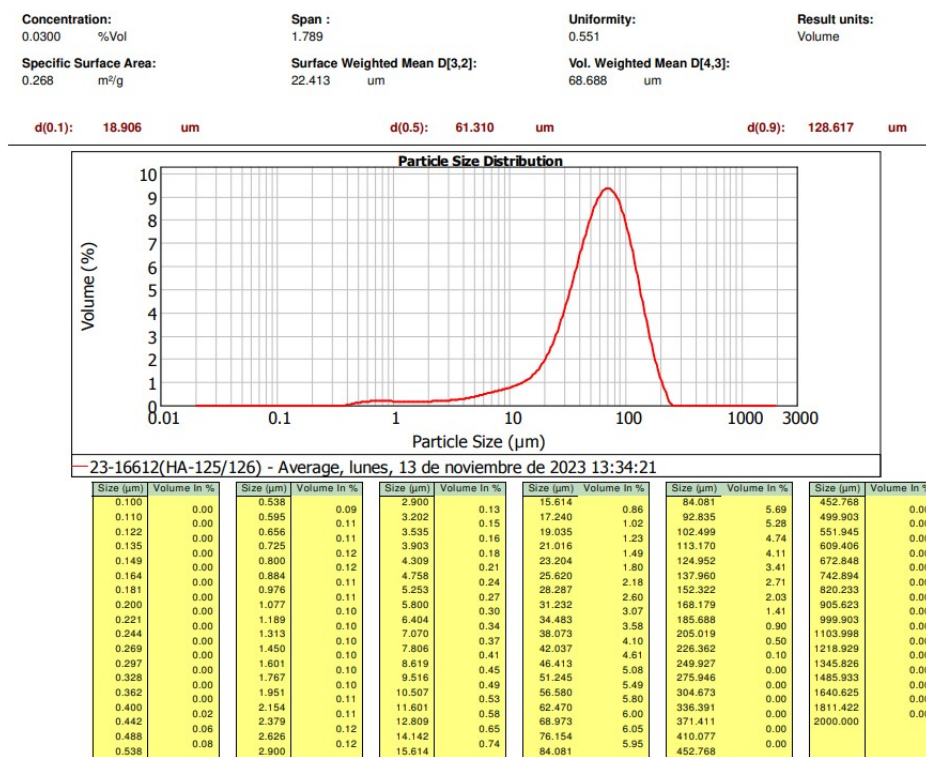


Figure S15. Particle size distribution of OS@MEMO.

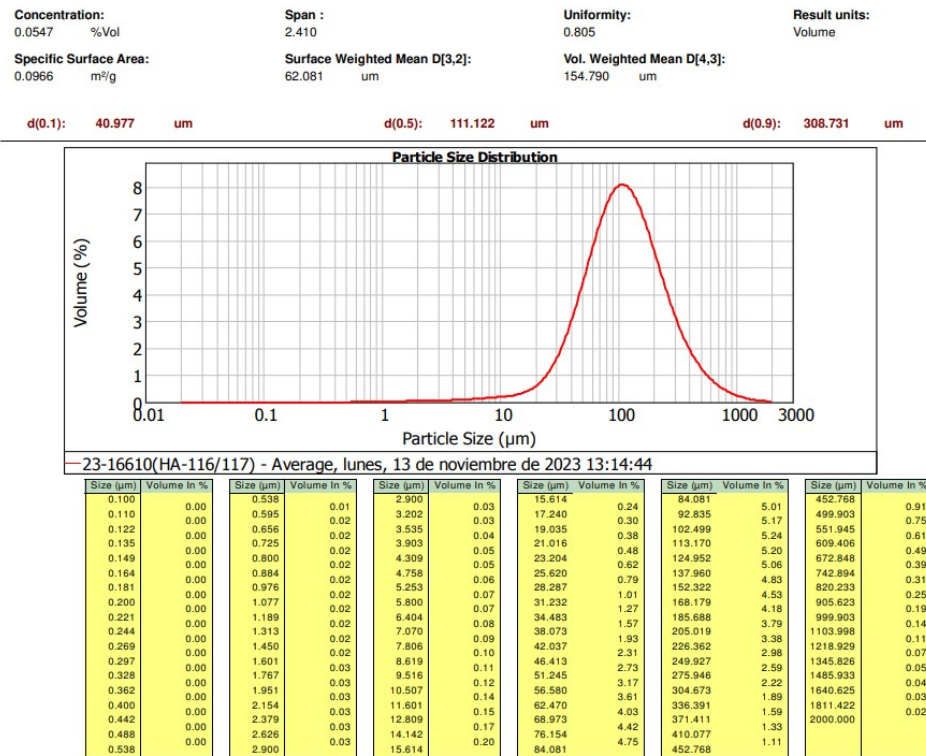


Figure S16. Particle size distribution of OS@ODTMS.

Table S3. Particle size distribution obtained with Granulometry assays.

	Feldspar	OS	OS@APTMS	OS@AEAPTMS	OS@MEMO	OS@ODTMS
d10 (μm)	1.463	13.783	40.596	93.996	18.906	40.977
d50 (μm)	9.059	57.434	82.350	192.235	69.310	111.122
d90 (μm)	25.554	124.692	171.012	541.559	128.617	308.731
D[3,2] (μm)	3.759	18.923	44.028	171.199	22.413	62.081
D[4,3] (μm)	11.561	64.734	126.312	277.906	68.688	154.790
Surf. Area (m^2/g)	1.601	0.317	0.136	0.035	0.268	0.0966
Uniformity	0.838	0.586	0.866	0.774	0.551	0.805

4. IR Spectra

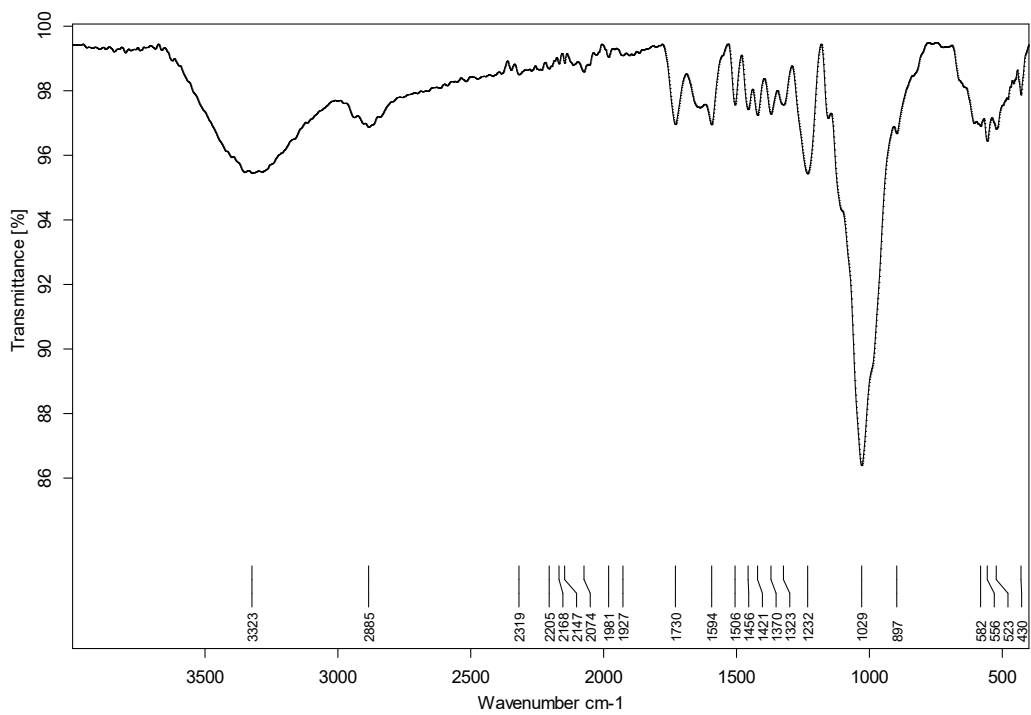


Figure S17. IR (ATR) spectra of OS.

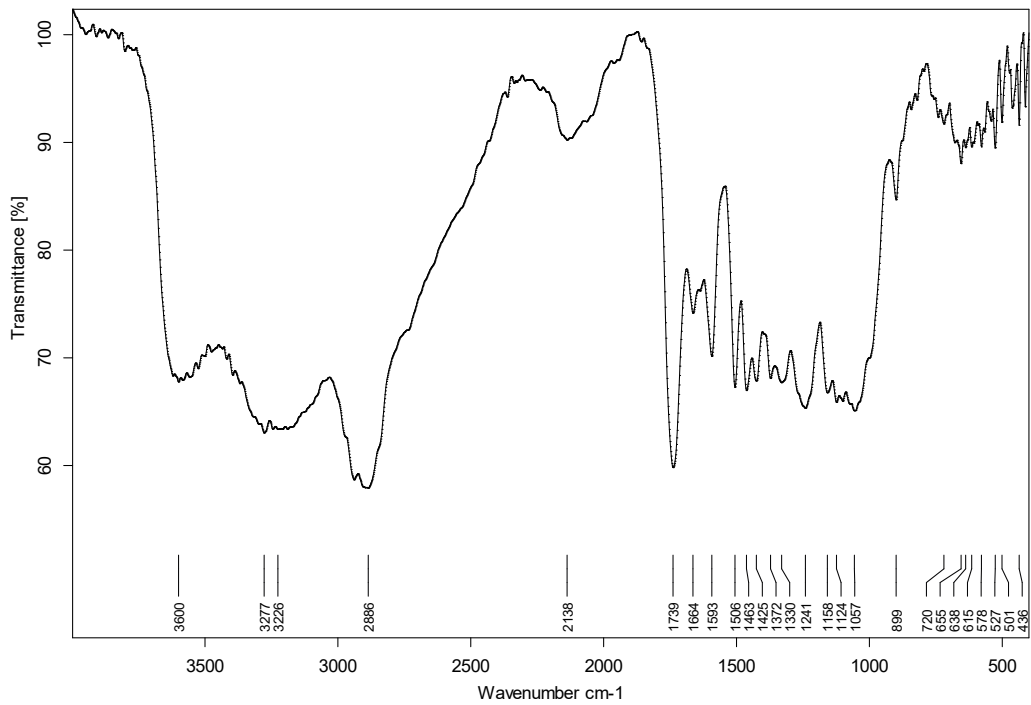


Figure S18. IR (DRIFT) spectra of OS.

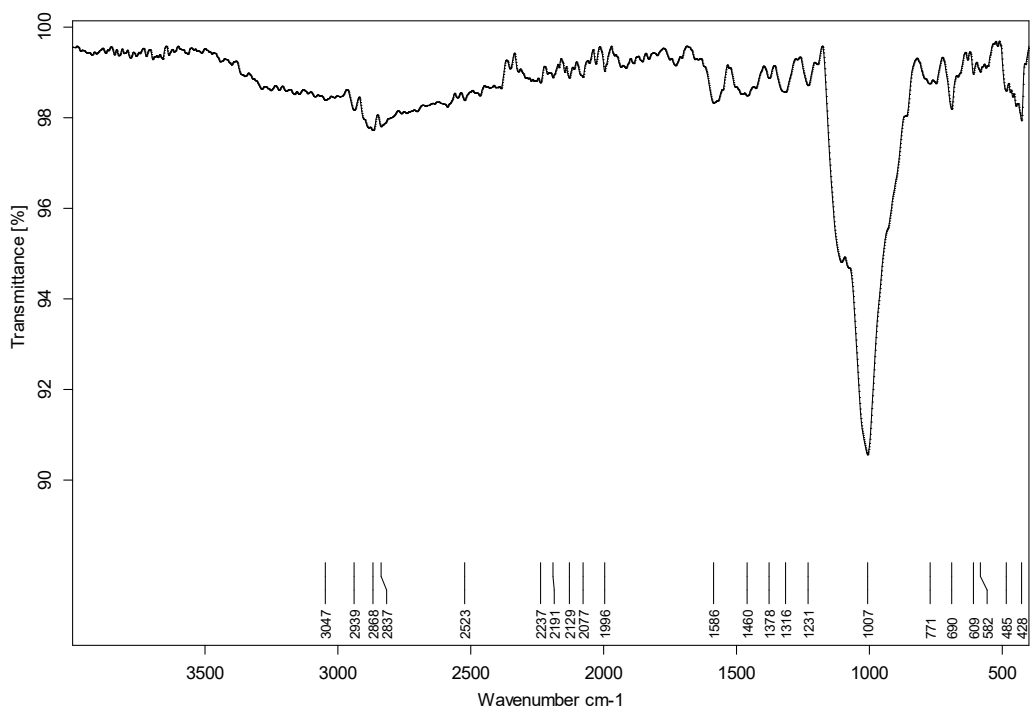


Figure S19. IR (ATR) spectra of OS@APTMS.

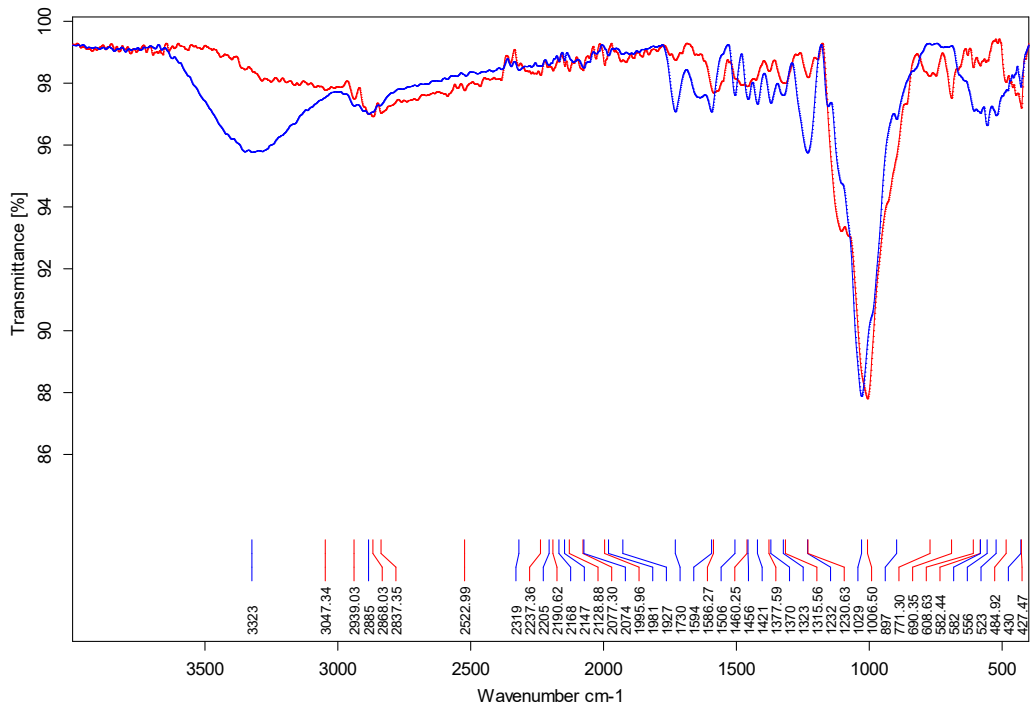


Figure S20. Comparation of IR (ATR) spectra of OS (blue) with OS@APTMS (red).

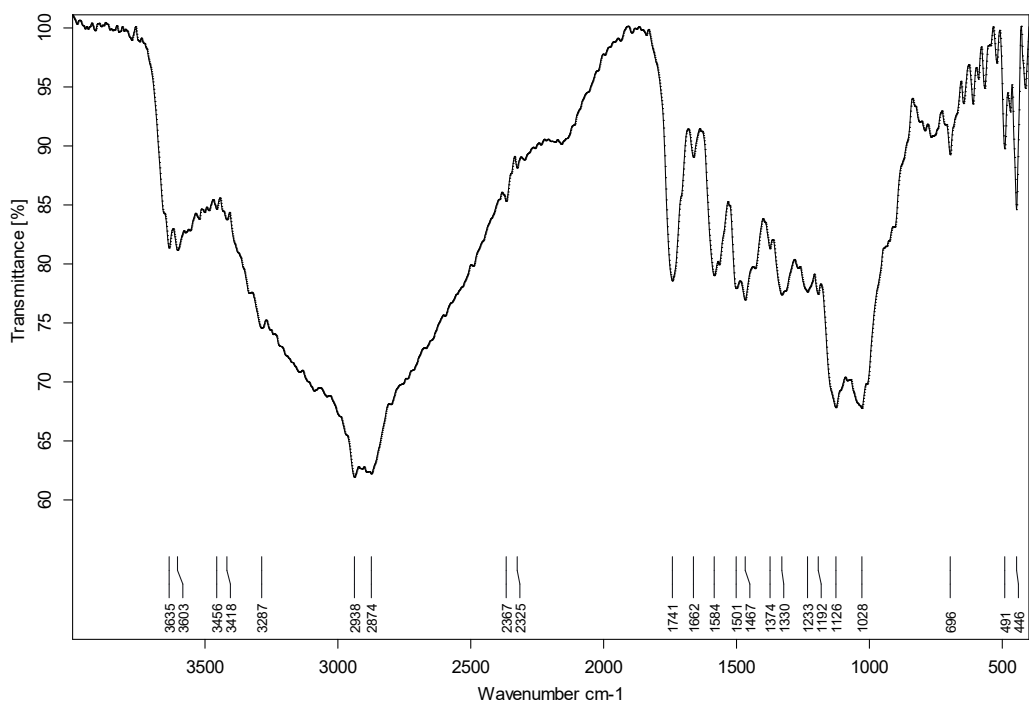


Figure S21. IR (DRIFT) spectra of OS@APTMS.

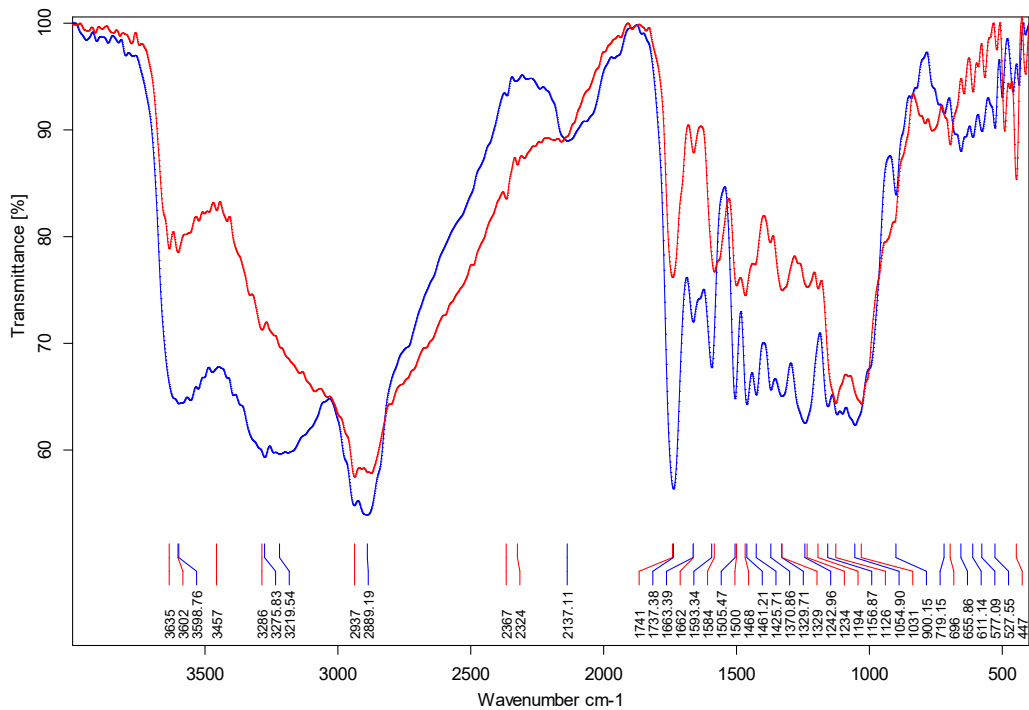


Figure S22. Comparison IR (DRIFT) spectra of OS (blue) and OS@APTMS (red).

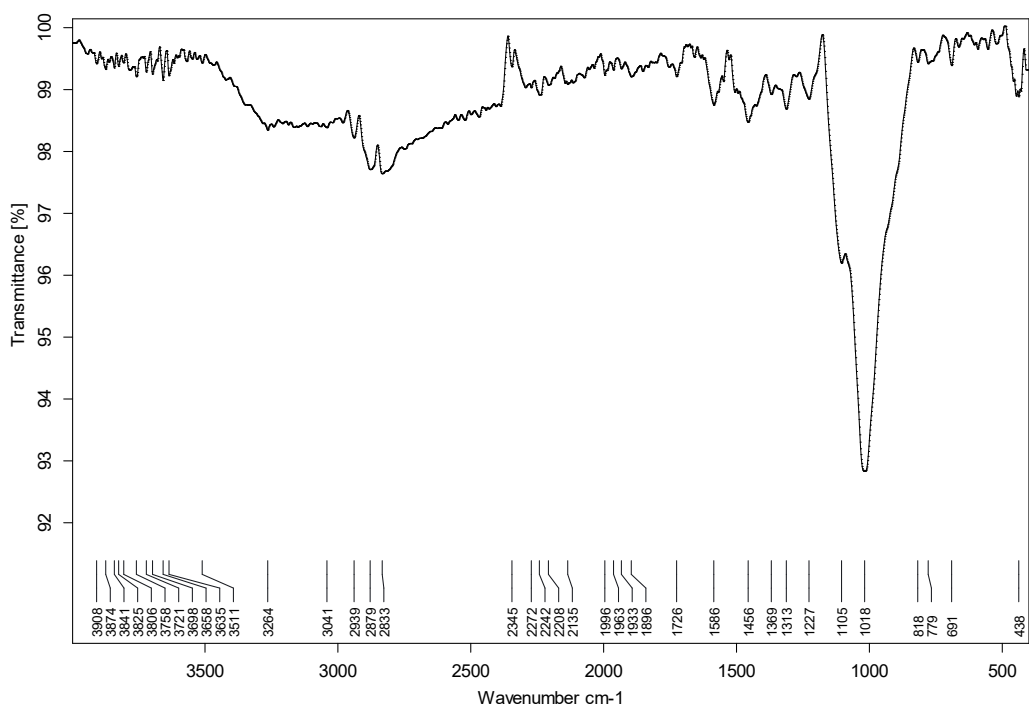


Figure S23. IR (ATR) spectra of OS@AEAPTMS.

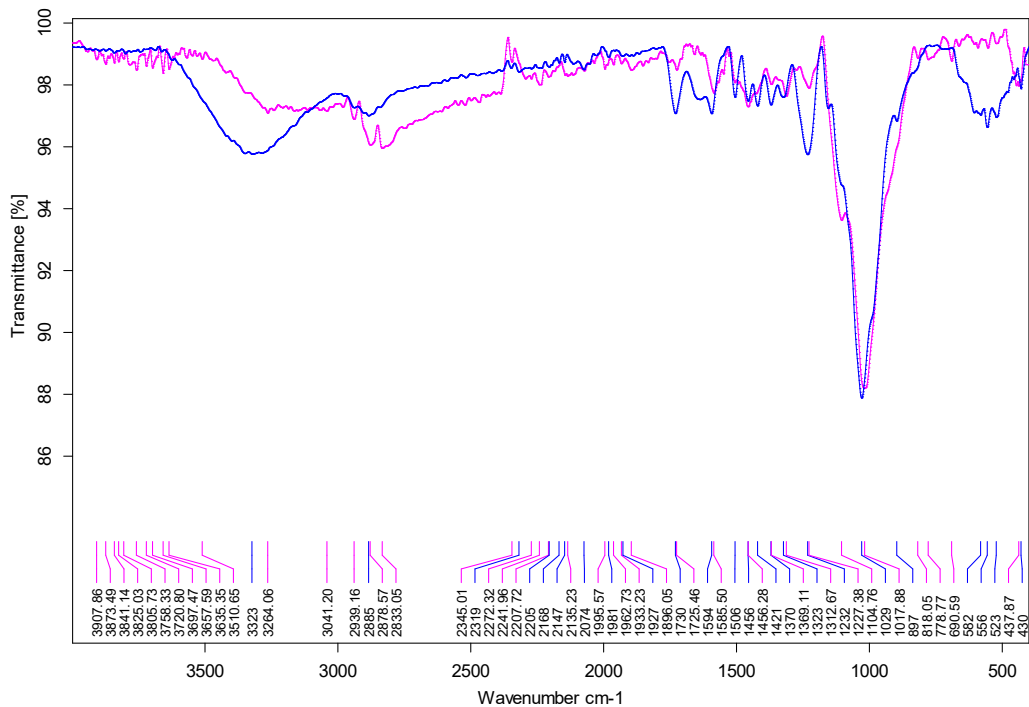


Figure S24. Comparation IR (ATR) spectra of OS (blue) with OS@AEAPTMS (pink).

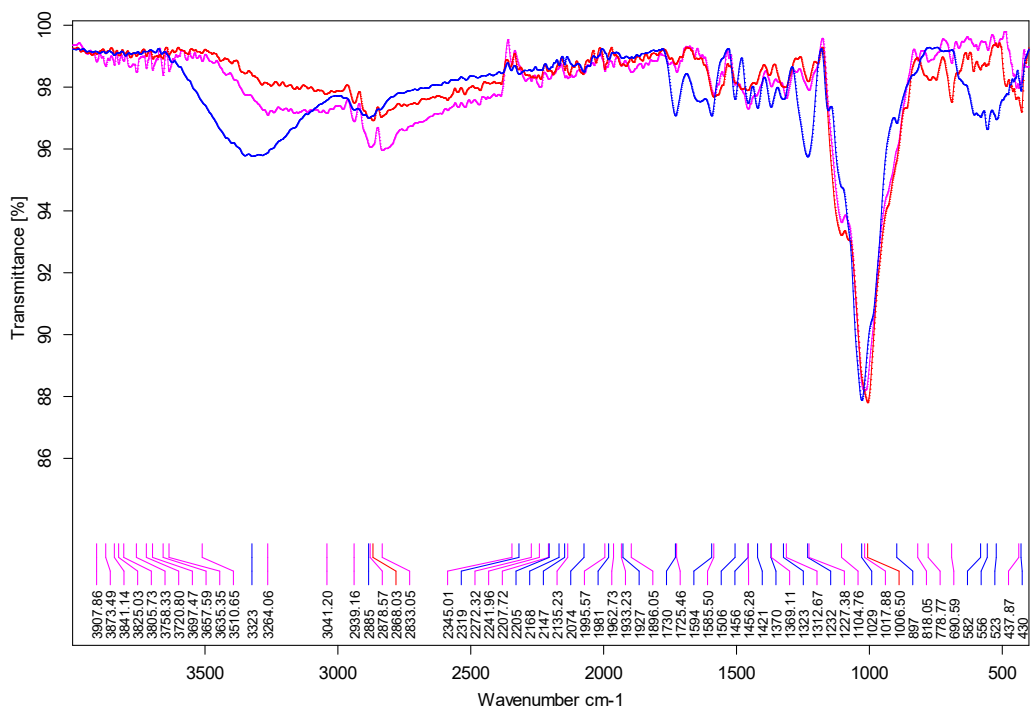


Figure S25. Comparation IR (ATR) spectra of OS (blue) with OS@APTMS (red) and OS@AEAPTMS (pink).

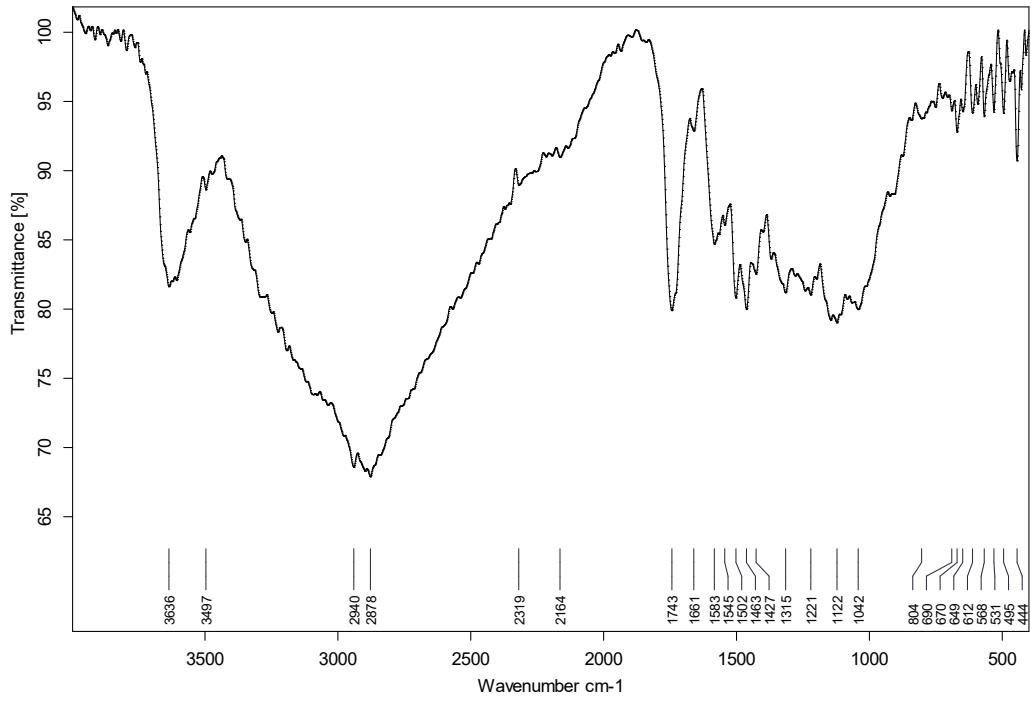


Figure S26. IR (DRIFT) spectra of virgin OS@AEAPTMS.

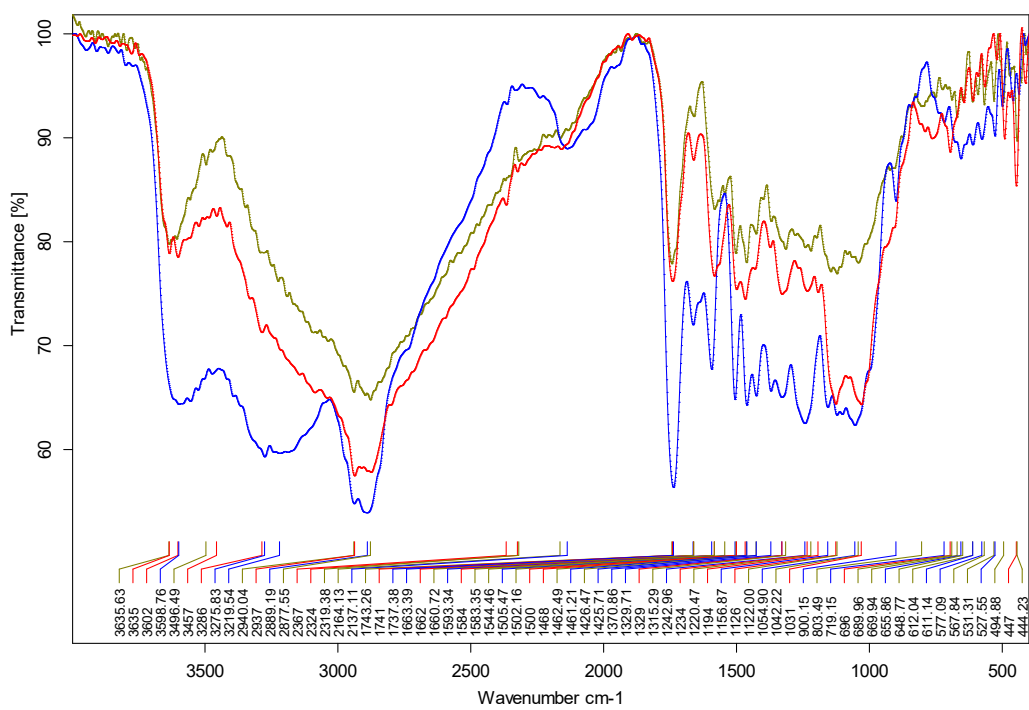


Figure S27. Comparation IR (DRIFT) spectra of OS (blue), OS@APTMS (red) and OS@AEAPTMS (green).

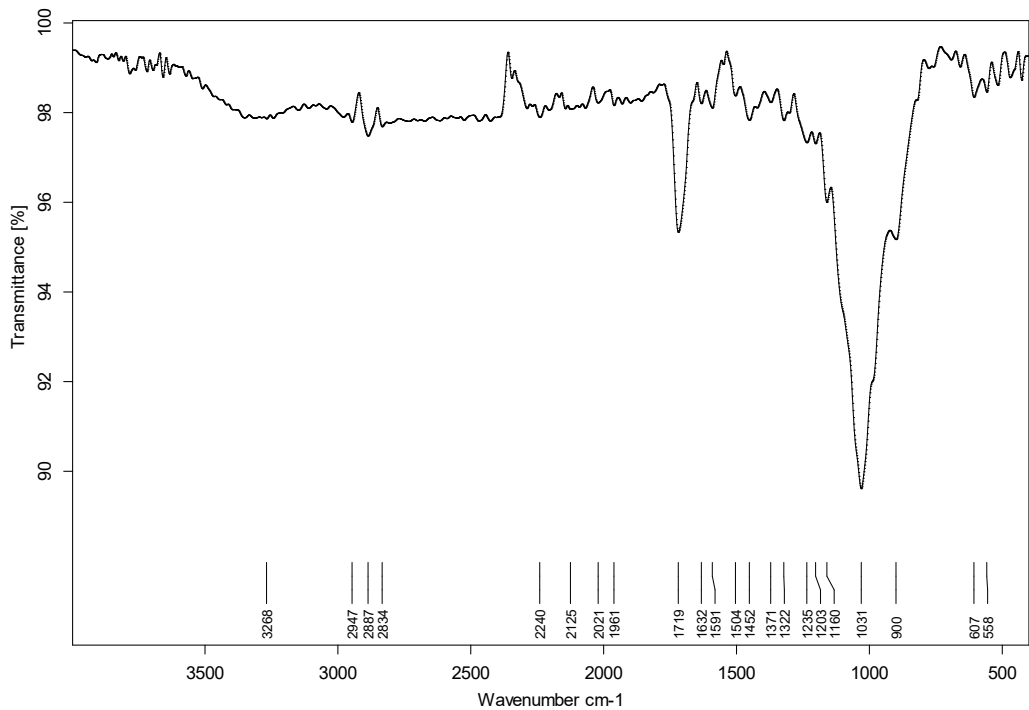


Figure S28. IR (ATR) spectra of OS@MEMO.

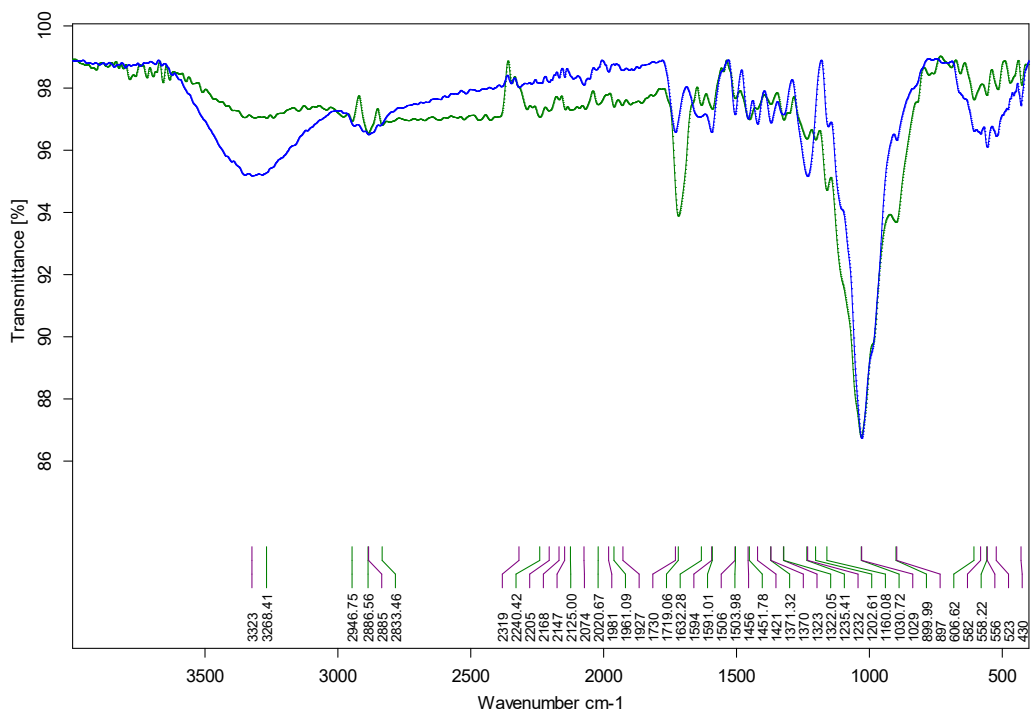


Figure S29. Comparation IR (ATR) spectra of OS (blue) and OS@MEMO (green).

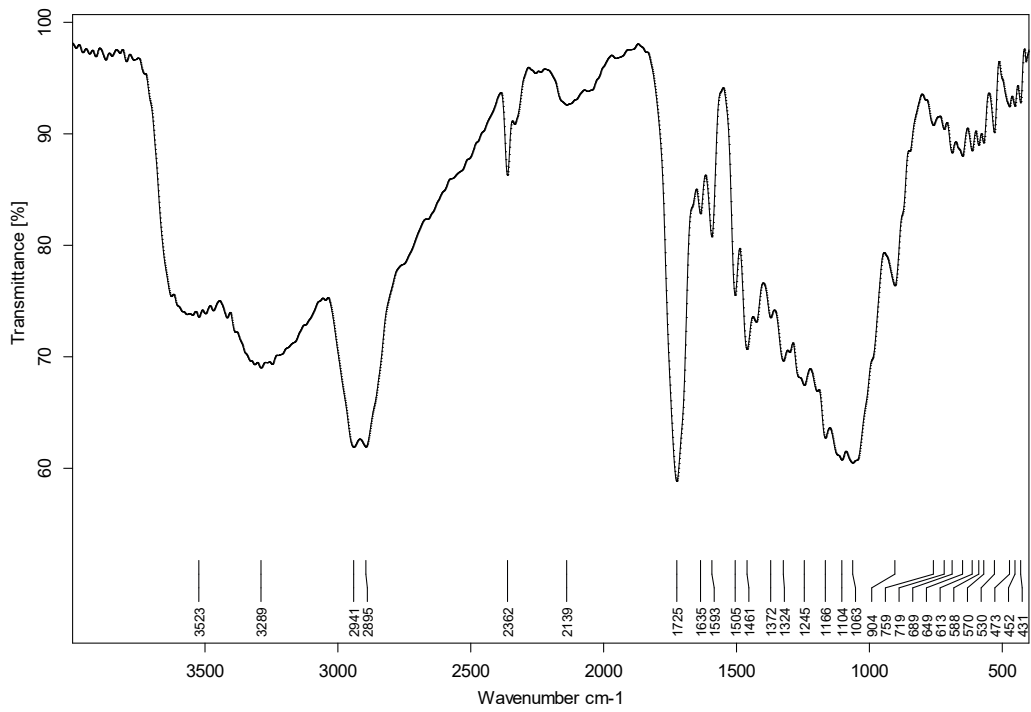


Figure S30. IR (DRIFT) spectra of OS@MEMO.

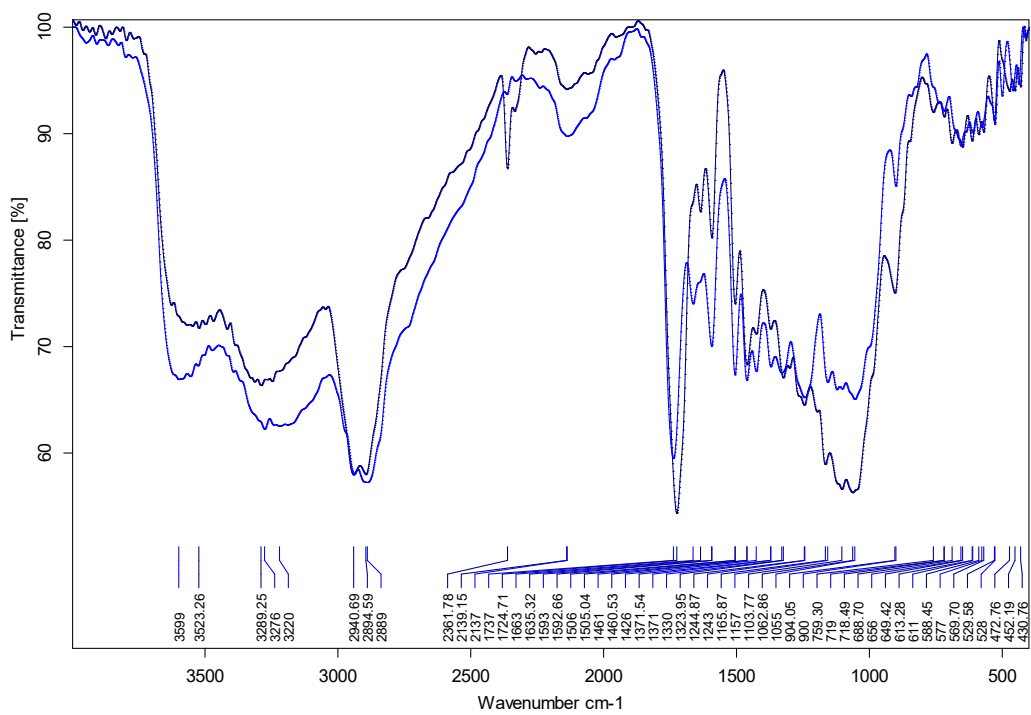


Figure S31. Comparation IR (DRIFT) spectra of OS (blue) and OS@MEMO (dark blue).

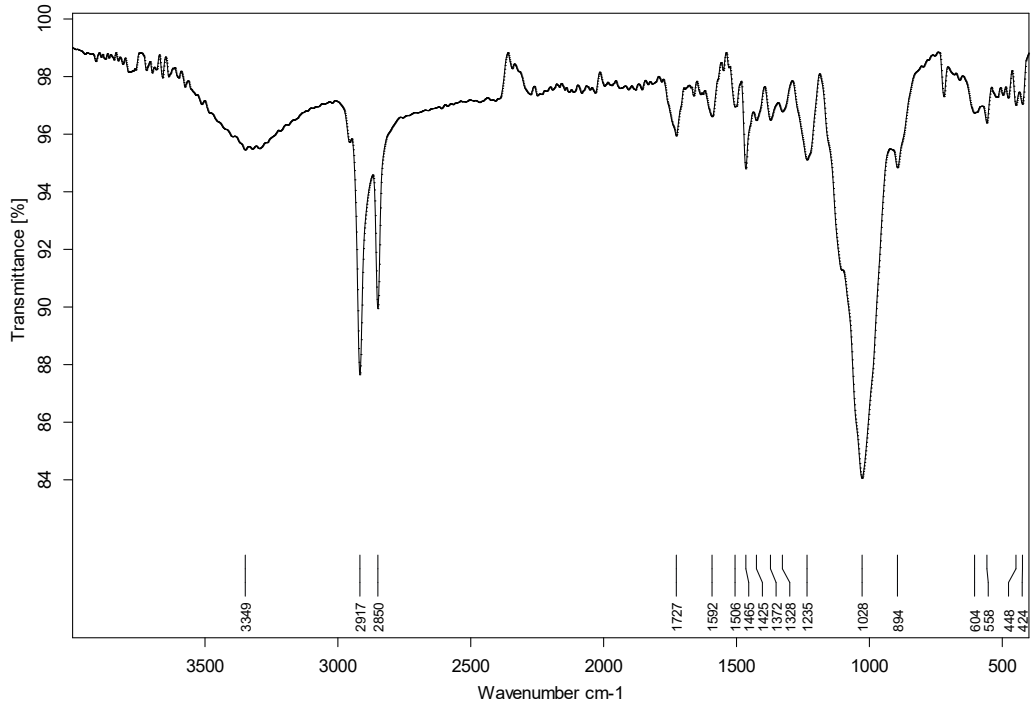


Figure S32. IR (ATR) spectra of virgin OS@ODTMS.

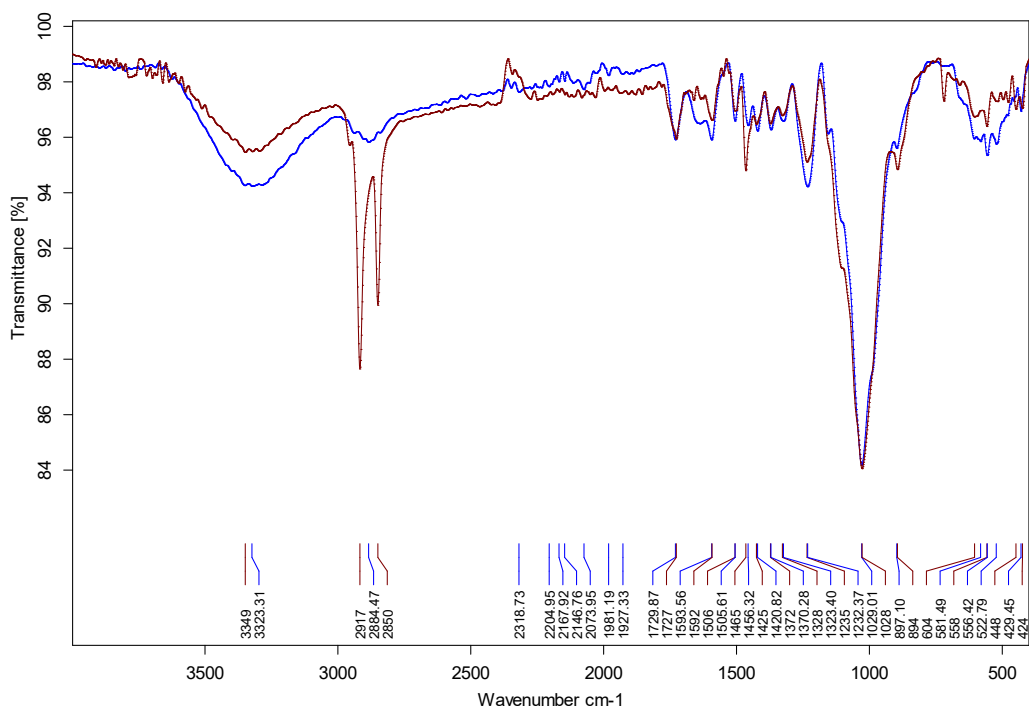


Figure S33. Comparation IR (ATR) spectra of OS (blue) and OS@ODTMS (brown).

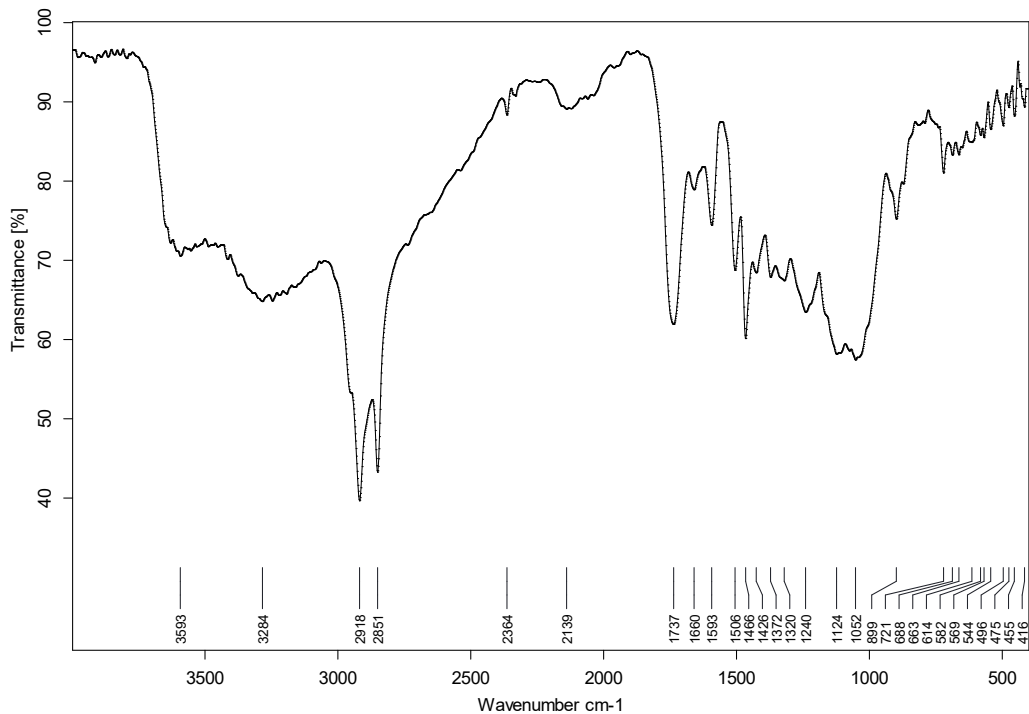


Figure S34. IR (DRIFT) spectra of virgin OS@ODTMS.

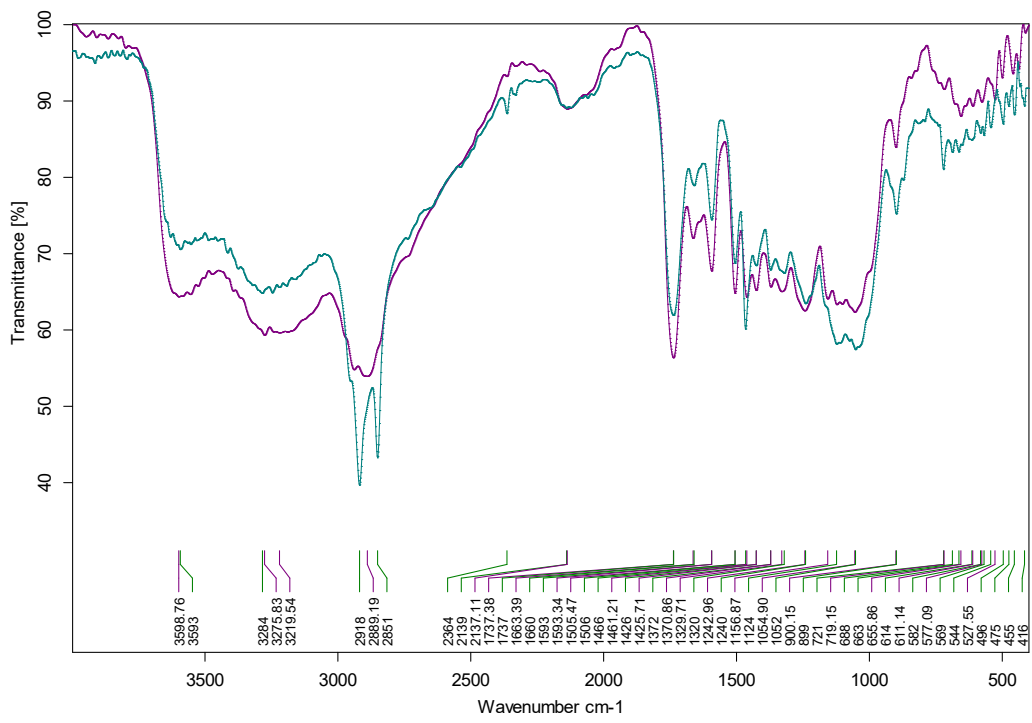


Figure S35. Comparation IR (DRIFT) spectra of OS (purple) and OS@ODTMS (green).

5. ζ -Potential and Electrophoretic mobility

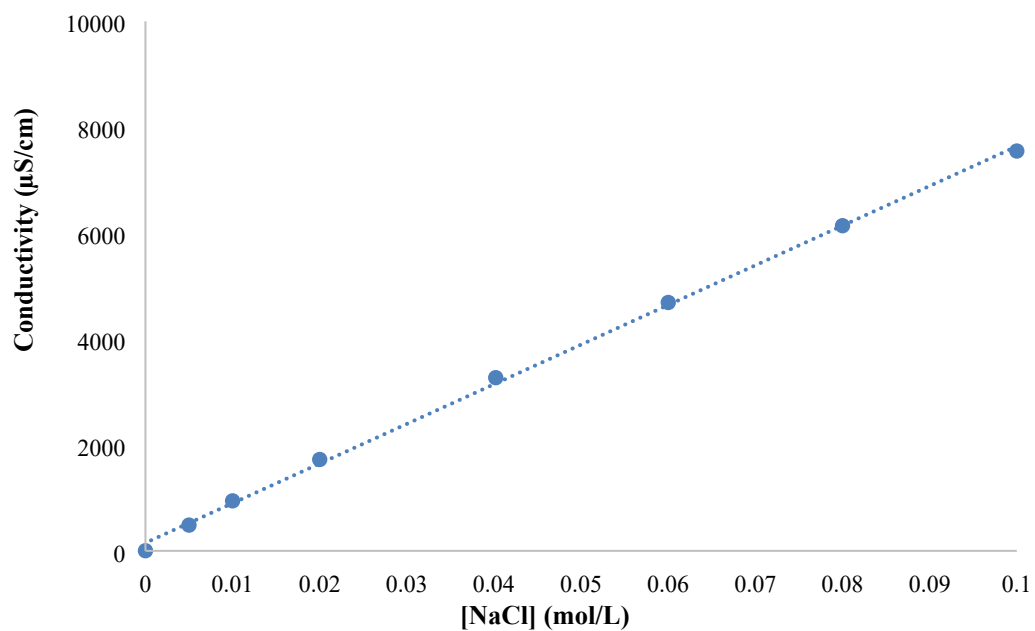


Figure S36. Calibration line of Conductivity ($\mu\text{S}/\text{cm}$) vs $[\text{NaCl}]$ (mol/L).

Table S4. Fraction suspended in water for the determination of the ζ -potential.

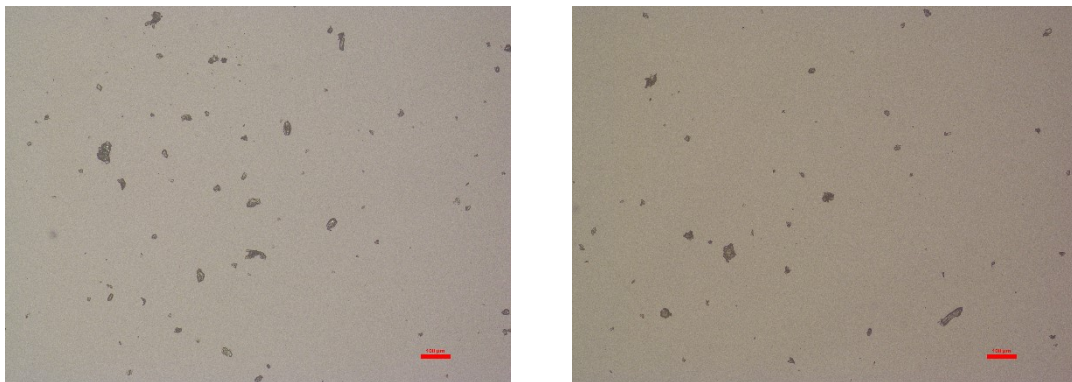
Entry	Material	% Fraction suspended
1	OS@APTMS	17
2	OS@AEAPTMS	17
3	OS@MEMO	34
4	OS@ODTMS	17
5	OS@APTMS	33

Table S5. Electrophoretic mobility and ζ -potential dependence with the pH of OS and OS@Silanized particles in water. Conductivity fixed at 700 $\mu\text{S}/\text{cm}$.

Sample	pH	Electroph. mobility ($\mu\text{m}\cdot\text{cm}/\text{Vs}$)	ζ -potential (mV)
OS	4	-1.32 \pm 0.06	-16.9 \pm 0.8
OS	5	-1.56 \pm 0.04	-19.9 \pm 0.6
OS	6	-1.67 \pm 0.05	-21.2 \pm 0.7
OS	7	-1.64 \pm 0.05	-21.0 \pm 0.7
OS	8	-1.78 \pm 0.05	-22.8 \pm 0.6
OS	9	-1.73 \pm 0.03	-22.1 \pm 1.0
OS	10	-1.75 \pm 0.03	-22.3 \pm 0.9
OS@APTMS	4	2.46 \pm 0.03	31.3 \pm 0.4
OS@APTMS	5	2.24 \pm 0.04	28.3 \pm 0.6
OS@APTMS	6	-0.14 \pm 0.07	-1.8 \pm 0.9
OS@APTMS	7	-0.37 \pm 0.04	-4.7 \pm 0.5
OS@APTMS	8	-0.50 \pm 0.01	-6.4 \pm 0.2
OS@APTMS	9	-1.14 \pm 0.04	-14.5 \pm 0.6
OS@APTMS	10	-1.98 \pm 0.03	-25.3 \pm 0.3
OS@AEAPTMS	4	2.47 \pm 0.02	31.5 \pm 0.2
OS@AEAPTMS	5	2.12 \pm 0.02	27.1 \pm 0.2
OS@AEAPTMS	6	1.50 \pm 0.02	19.2 \pm 0.2
OS@AEAPTMS	7	0.60 \pm 0.03	7.6 \pm 0.3
OS@AEAPTMS	8	-0.22 \pm 0.04	-2.8 \pm 0.4
OS@AEAPTMS	9	-1.26 \pm 0.07	-16.1 \pm 0.8
OS@AEAPTMS	10	-1.55 \pm 0.03	-19.8 \pm 0.4
OS@MEMO	4	-0.43 \pm 0.03	-5.5 \pm 0.3
OS@MEMO	5	-0.91 \pm 0.02	-11.7 \pm 0.3
OS@MEMO	6	-1.35 \pm 0.07	-17.2 \pm 0.9
OS@MEMO	7	-1.33 \pm 0.04	-16.9 \pm 0.5
OS@MEMO	8	-2.26 \pm 0.07	-28.8 \pm 0.9
OS@MEMO	9	-2.14 \pm 0.07	-27.3 \pm 0.9
OS@MEMO	10	-2.68 \pm 0.07	-34.2 \pm 0.9
OS@ODTMS	4	-0.75 \pm 0.07	-9.6 \pm 0.8
OS@ODTMS	5	-1.30 \pm 0.04	-16.6 \pm 0.6

OS@ODTMS	6	-1.53 ± 0.10	-19.5 ± 1.3
OS@ODTMS	7	-1.26 ± 0.10	-16.1 ± 1.3
OS@ODTMS	8	-1.48 ± 0.15	-18.9 ± 1.9
OS@ODTMS	9	-1.85 ± 0.10	-23.6 ± 1.2
OS@ODTMS	10	-2.85 ± 0.18	-36.4 ± 2.3

6. Particle size distribution of deposited and suspended OS and OS@Silanized biofillers



Suspended fraction OS

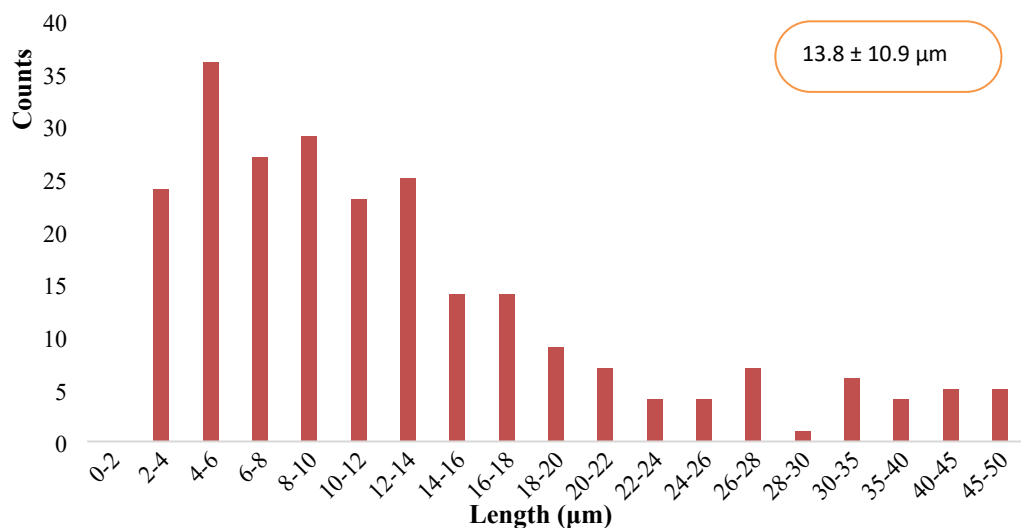
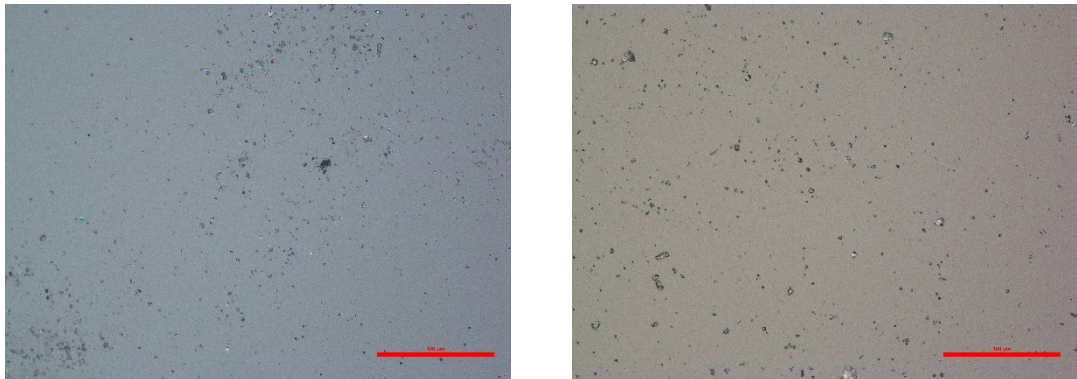


Figure S37. Optical images and particle size distribution (an overall of 250 particles) of initial virgin OS material in the fraction steadily suspended in water (about a 17% of the total amount), determined from optical microscopy.



Suspended fraction OS@APTMS

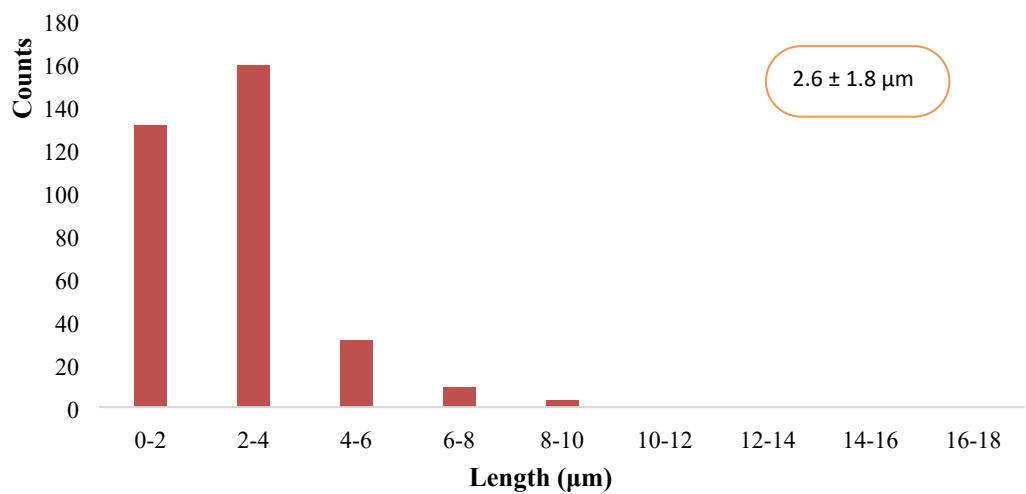
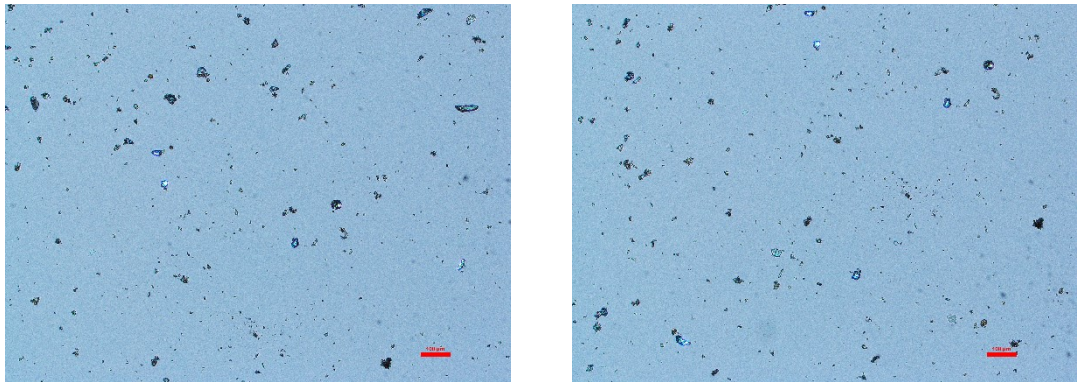


Figure S38. Optical images and particle size distribution (an overall of 250 particles) of OS@APTMS material in the fraction steadily suspended in water (about a 17% of the total amount), determined from optical microscopy.



Suspended fraction OS@AEAPTMS

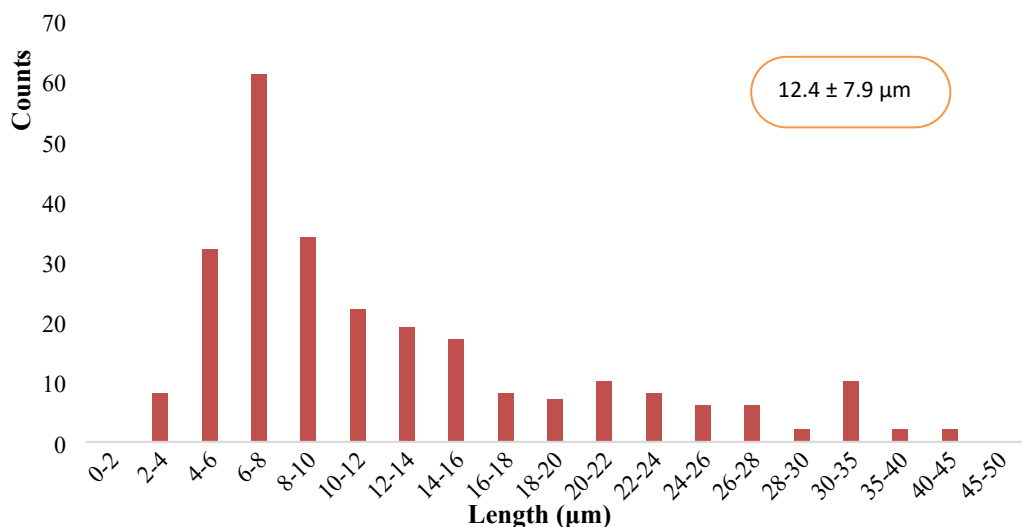
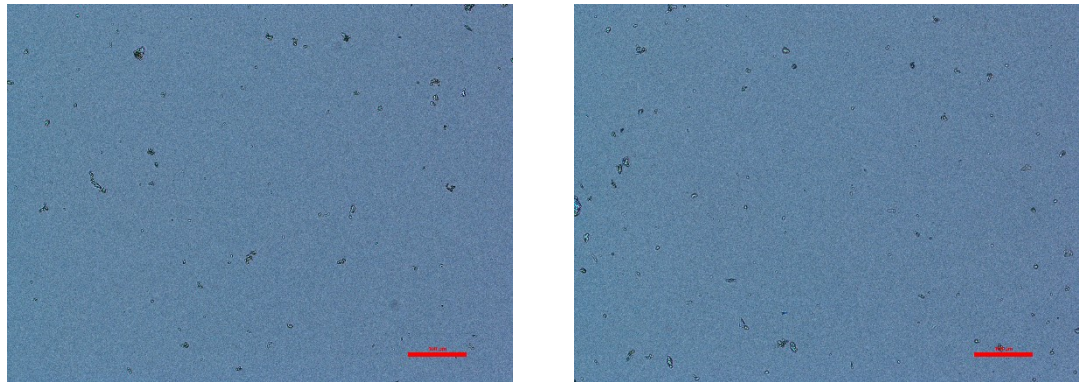


Figure S39. Optical images and particle size distribution (an overall of 250 particles) of OS@AEAPTMS material in the fraction steadily suspended in water (about a 34% of the total amount), determined from optical microscopy.



Suspended fraction OS@MEMO

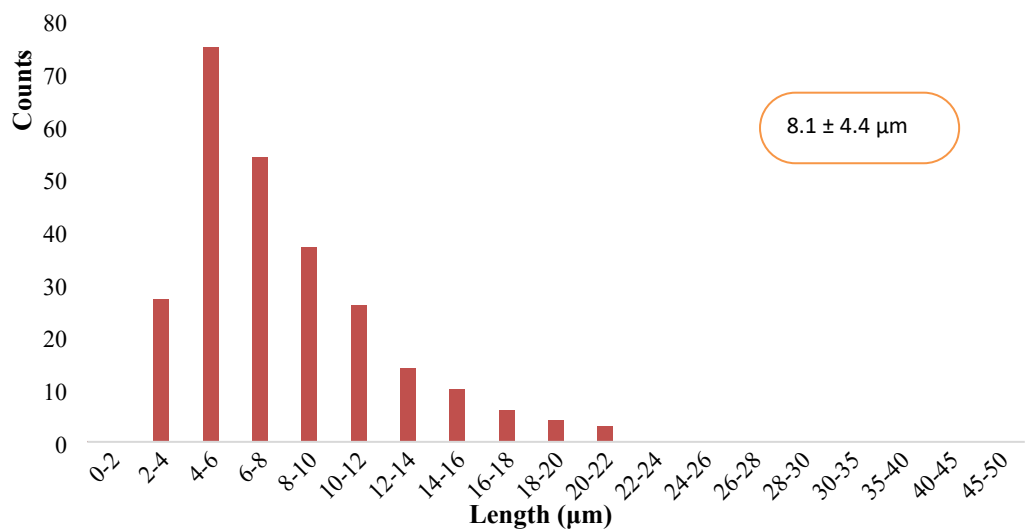
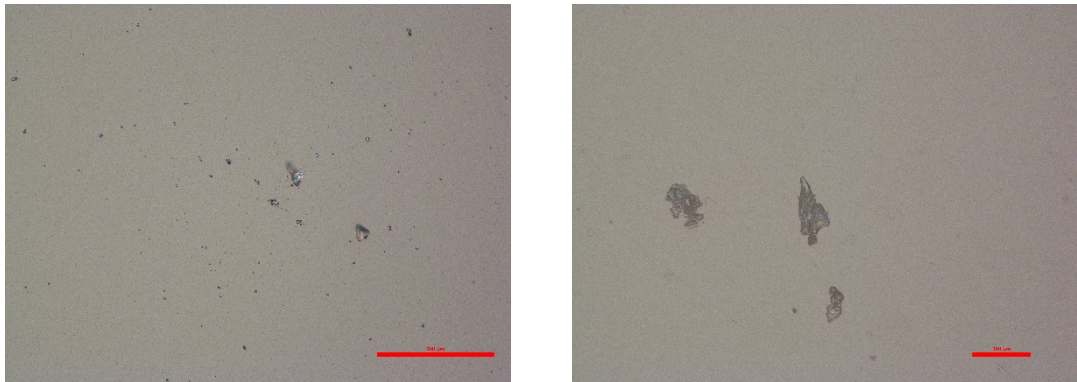


Figure S40. Optical images and particle size distribution (an overall of 250 particles) of OS@MEMO material in the fraction steadily suspended in water (about a 17% of the total amount), determined from optical microscopy.



Suspended fraction OS@ODTMS

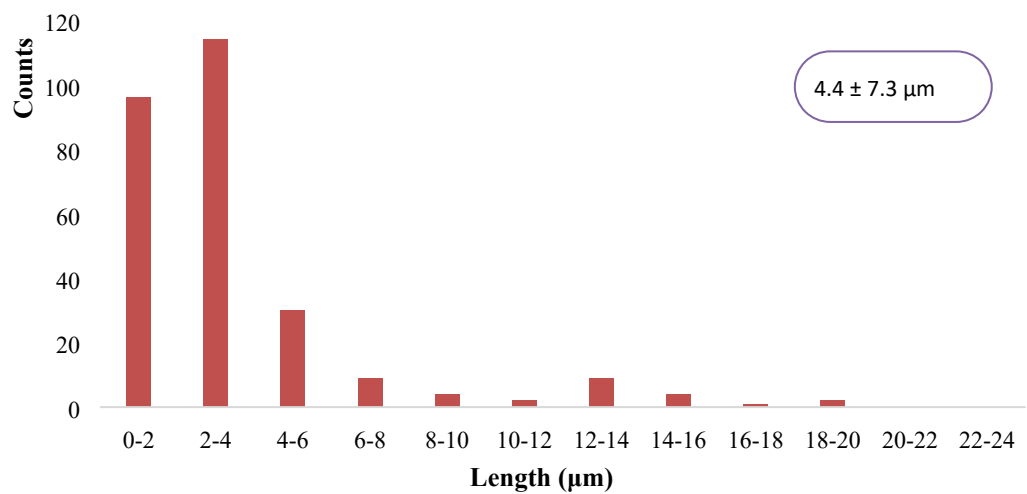
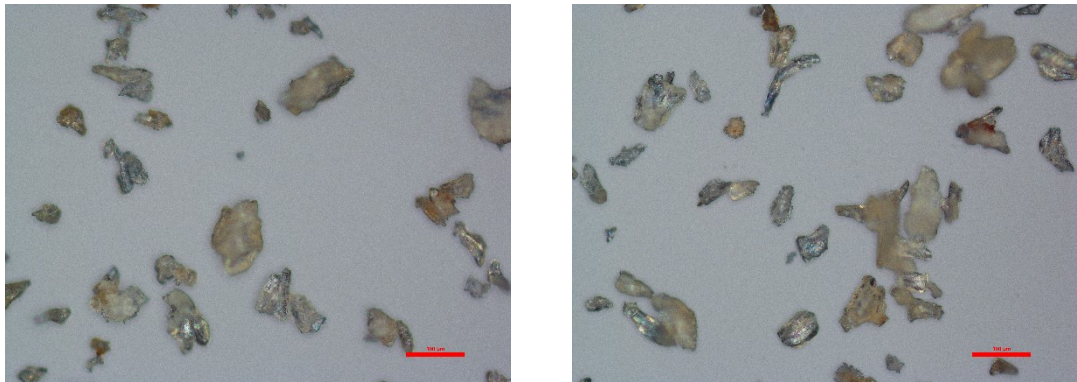


Figure S41. Optical images and particle size distribution (an overall of 250 particles) of OS@ODTMS material in the fraction steadily suspended in water (about a 33% of the total amount), determined from optical microscopy.



Deposited fraction OS

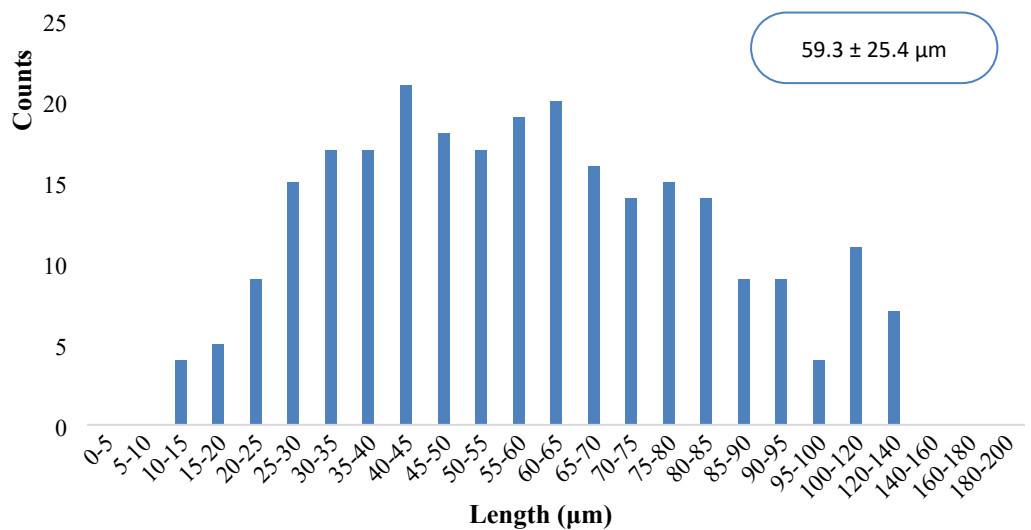
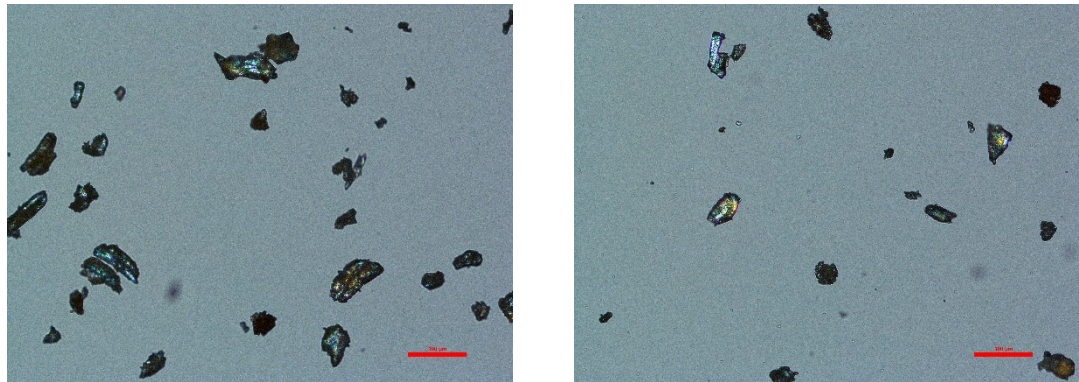


Figure S42. Optical images and particle size distribution (an overall of 250 particles) in the deposited fraction of initial virgin OS material (about a 83% of the total amount), determined from optical microscopy.



Deposited fraction OS@APTMS

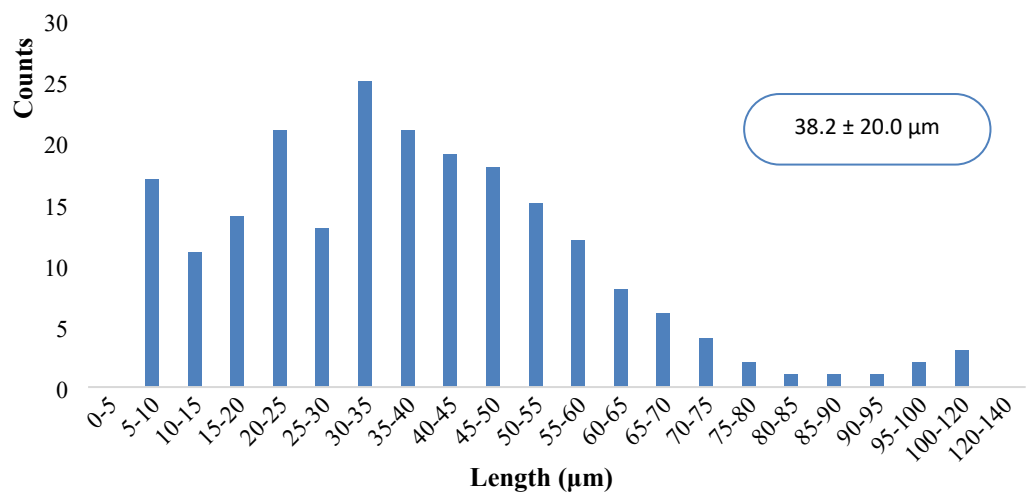


Figure S43. Optical images and particle size distribution (an overall of 250 particles) in the deposited fraction of OS@APTMS material (about a 83% of the total amount), determined from optical microscopy.

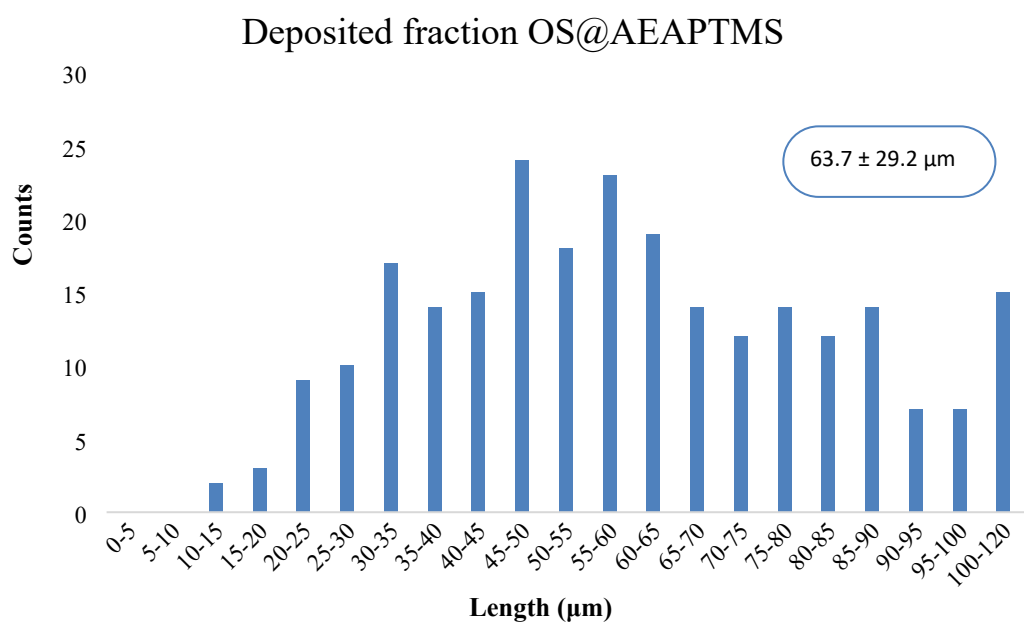
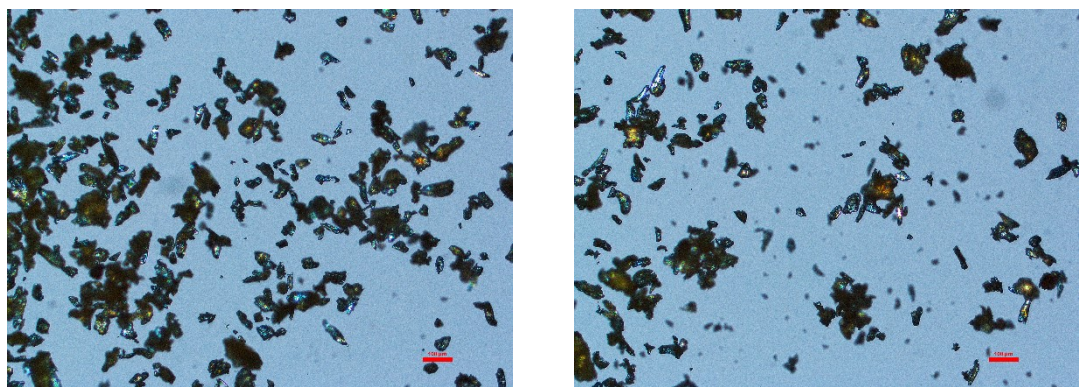
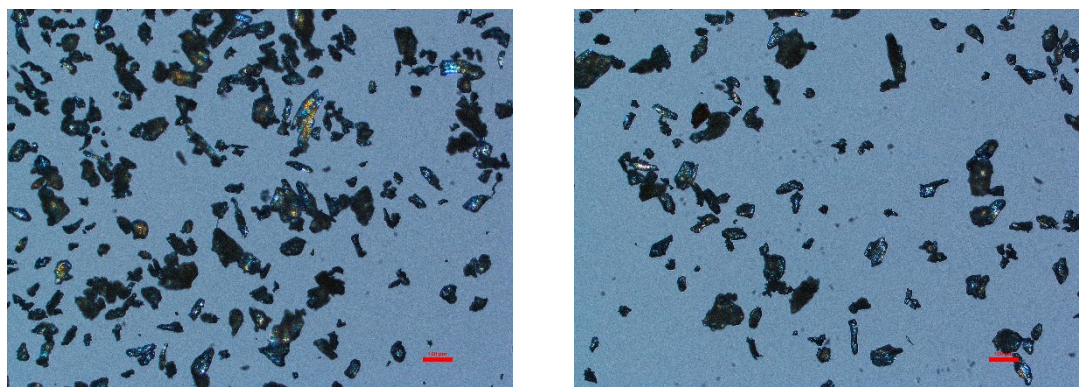


Figure S44. Optical images and particle size distribution (an overall of 250 particles) in the deposited fraction of OS@AEAPTMS material (about a 66% of the total amount), determined from optical microscopy.



Deposited fraction OS@MEMO

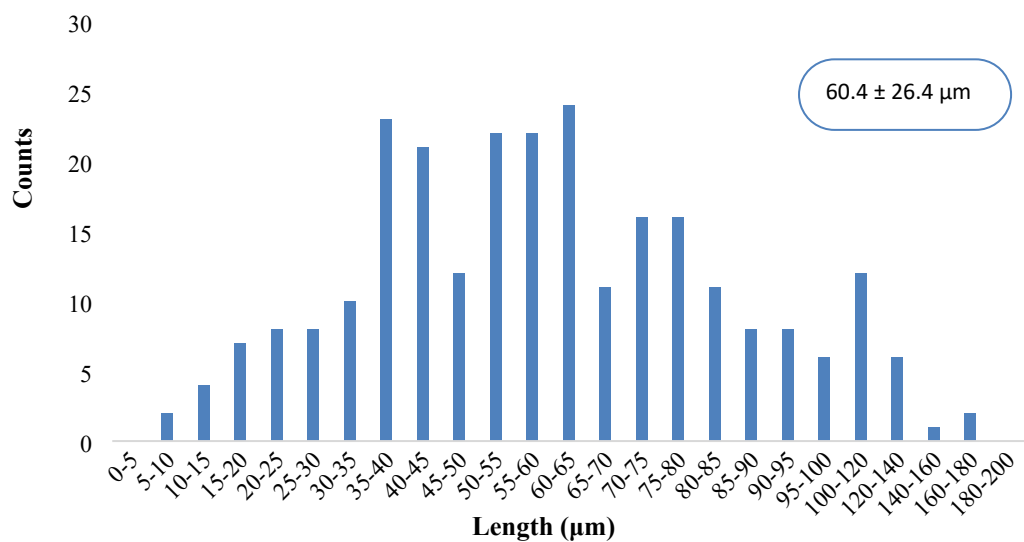
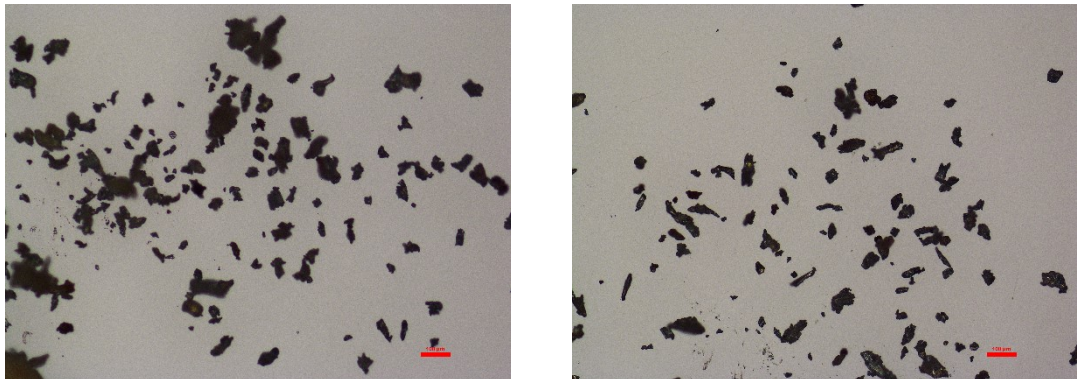


Figure S45. Optical images and particle size distribution (an overall of 250 particles) in the deposited fraction of OS@MEMO material (about a 83% of the total amount), determined from optical microscopy.



Deposited fraction OS@ODTMS

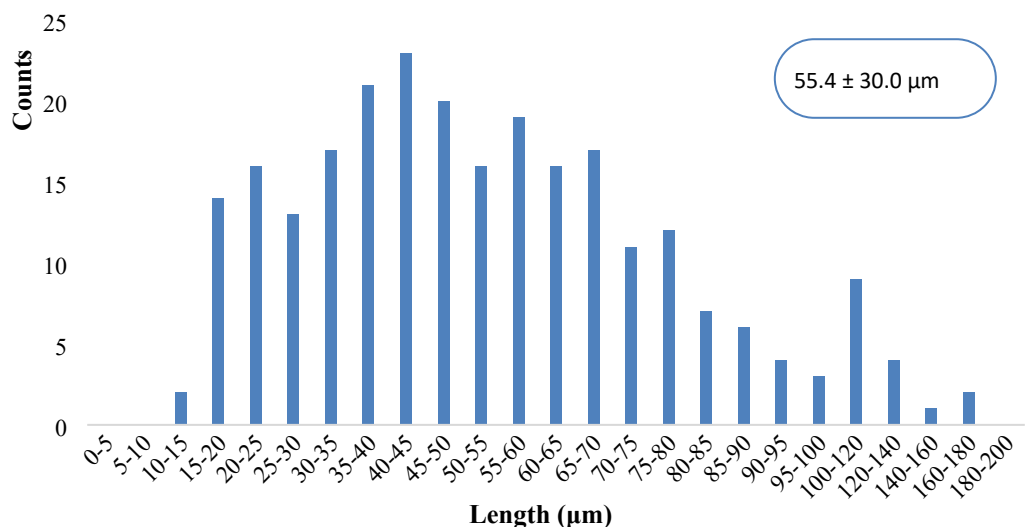


Figure S46. Optical images and particle size distribution (an overall of 250 particles) in the deposited fraction of OS@ODTMS material (about a 67% of the total amount), determined from optical microscopy.

7. Mechanical properties

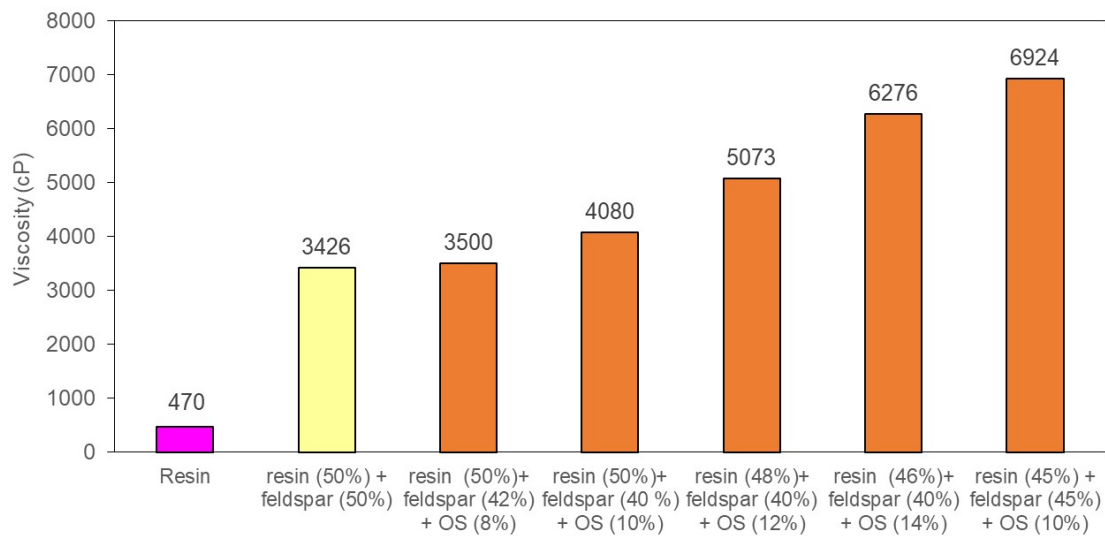


Figure S47. Optimization of resin/feldspar/OS ratio (% w/w) using viscosity measurements.

Table S6. Flexural modulus (MPa), Flexural strength (MPa), Storage modulus (E') at 25 °C (MPa) and glass transition temperatures (°C) of the resulting composites.

Sample	Flexural modulus (MPa)	Flexural strength (MPa)	Storage modulus at 25 °C (MPa)	Tan δ peak (T_g °C)
Resin (50%) + Feldspar (50%)	4614 ± 53	84 ± 7	612.6	82.1
Resin (50%) + Feldspar (42%) + OS (8%)	4519 ± 107	58 ± 5	569.7	80.5
Resin (50%) + Feldspar (42%) + OS@APTMS (8%)	5020 ± 241	62 ± 3	609.3	86.1
Resin (50%) + Feldspar (42%) + OS@AEAPTMS (8%)	4801 ± 77	59 ± 4	645.8	82.9
Resin (50%) + Feldspar (42%) OS@MEMO (8%)	5249 ± 166	56 ± 10	639.6	84.0
Resin (50%) + Feldspar (42%) + OS@ODTMS (8%)	4341 ± 53	41 ± 1	771.2	84.6

Table S7. Viscosity values and Barcol hardness determined for different mixtures and cured composites.

Entry	Mixture	Viscosity (cP) ^a	Hardness (B) ^a
1	Resin	470 ± 6	22.7 ± 1.8
2	Resin (50%) + Feldspar (50%)	3426 ± 16	55.2 ± 1.6
3	Resin (50%) + Feldspar (42%) + OS (8%)	3500 ± 100	58.6 ± 1.4
4	Resin (50%) + Feldspar (40 %) +OS (10%)	4080 ± 140	58.7 ± 1.4
5	Resin (48%) + Feldspar (40%) + OS (12%)	5073 ± 15	57.3 ± 1.9
6	Resin (46%) + Feldspar (40%) + OS (14%)	6276 ± 24	55.9 ± 1.8
7	Resin (45%) + Feldspar (45%) + OS (10%)	6924 ± 12	53.5 ± 2.4
8	Resin (50%) + Feldspar (42%) + OS@APTMS (8%)	3118 ± 28	56.9 ± 2.0
9	Resin (50%) + Feldspar (42%) + OS@AEAPTMS (8%)	3048 ± 24	49.0 ± 3.0
10	Resin (50%) + Feldspar (42%) + OS@MEMO (8%)	4707 ± 112	56.3 ± 2.0
11	Resin (50%) + Feldspar (42%) + OS@ODTMS (8%)	3522 ± 42	36.0 ± 4.0

^a 250 mL vessel was filled with the mixtures and thermostated at 25 °C for 15 minutes, ensuring that no bubbles remain inside. The appropriate spindle was selected and immersed to its corresponding mark. The measurement was considered adequate when the torque was as close as possible to 50% and the measurements were carried out per triplicate.

8. Colorimetry

Table S8. Surface luminosity, chromaticity, aberrations and color difference of the resulting composites.

	Color (L*a*b*)	ΔL*	Δa*	Δb*	ΔE ^a
Resin (50%) + Feldspar (50%)	50.8 ± 0.6 0.67 ± 0.05 -4.8 ± 0.4				
Resin (50%) + Feldspar (42%) + OS (8%)	39.1 ± 0.2 3.49 ± 0.10 12.43 ± 0.43	-11.7	2.82	17.23	21.0
Resin (50%) + Feldspar (42%) + OS@APTMS (8%)	36.9 ± 2.3 5.00 ± 0.50 14.3 ± 1.1	-13.9	4.33	19.1	24.0
Resin (50%) + Feldspar (42%) + OS@AEAPTMS (8%)	34.4 ± 0.2 6.05 ± 0.13 14.0 ± 0.6	-16.42	5.38	18.8	25.5
Resin (50%) + Feldspar (42%) + OS@MEMO (8%)	41.1 ± 0.5 4.41 ± 0.08 15.1 ± 0.4	-9.7	3.74	19.9	22.5
Resin (50%) + Feldspar (42%) + OS@ODTMS (8%)	44.7 ± 0.1 5.07 ± 0.08 16.1 ± 0.4	-6.09	4.4	20.9	22.2

^a Mean values were calculated using the following formula $\Delta E = [(\Delta L^*)^2 + (\Delta a^*)^2 + (\Delta b^*)^2]^{1/2}$.

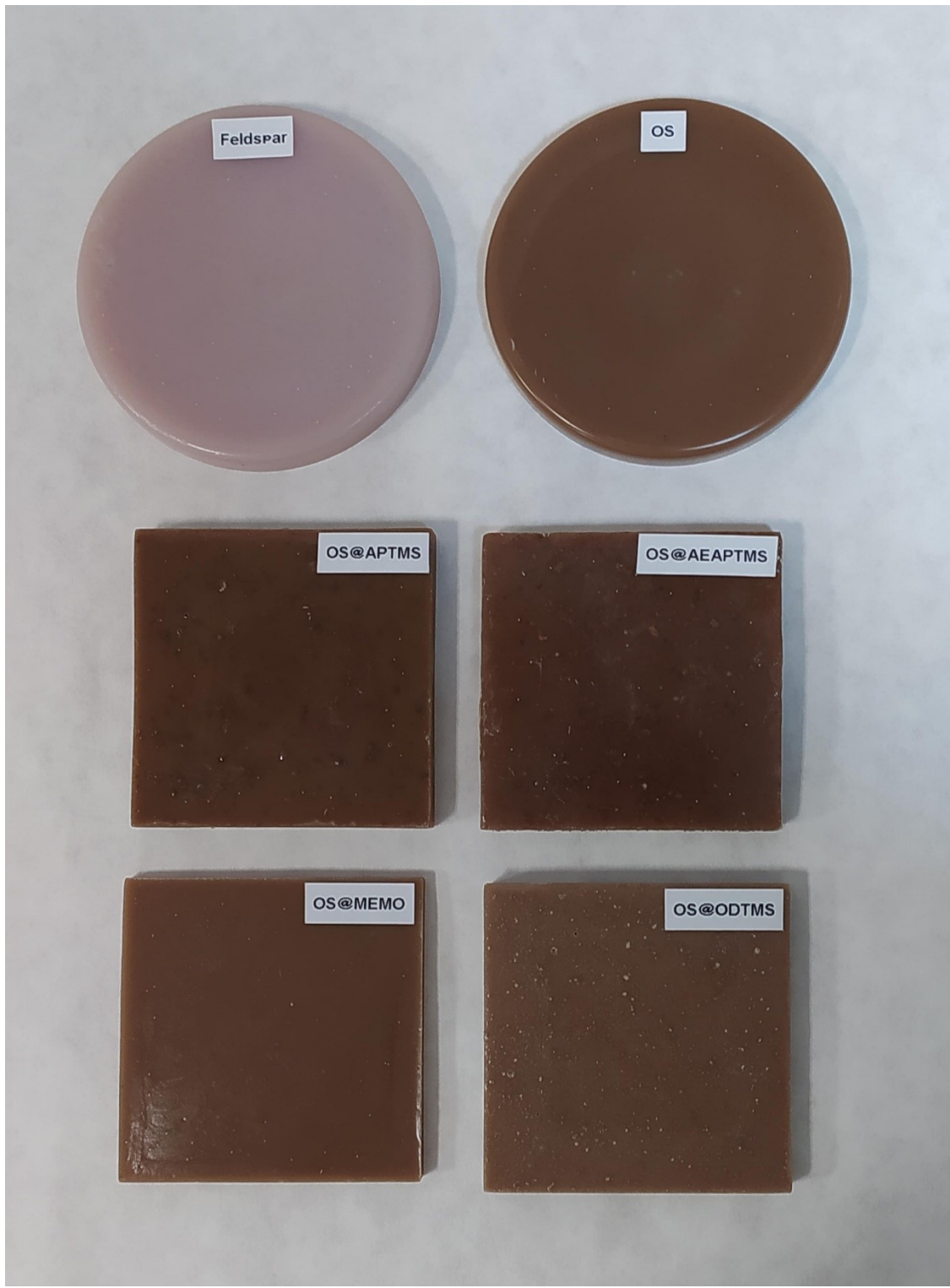


Figure S48. Composite probes of the two controls (pure resin and sodium feldspar) and those containing OS biofillers.

9. SEM images

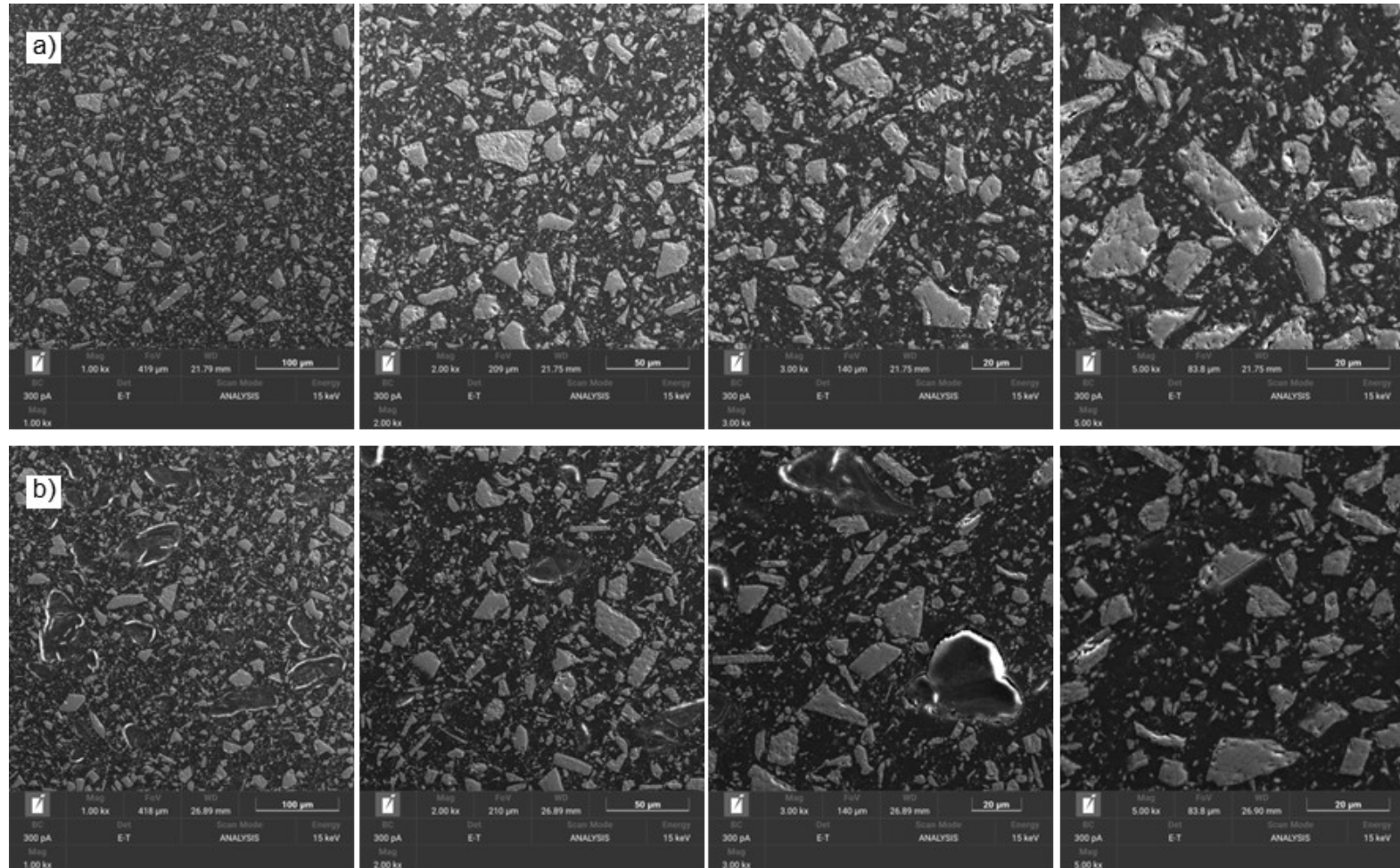


Figure S49. SEM micrographs showing the microstructure of the composites containing: a) feldspar; and b) OS.

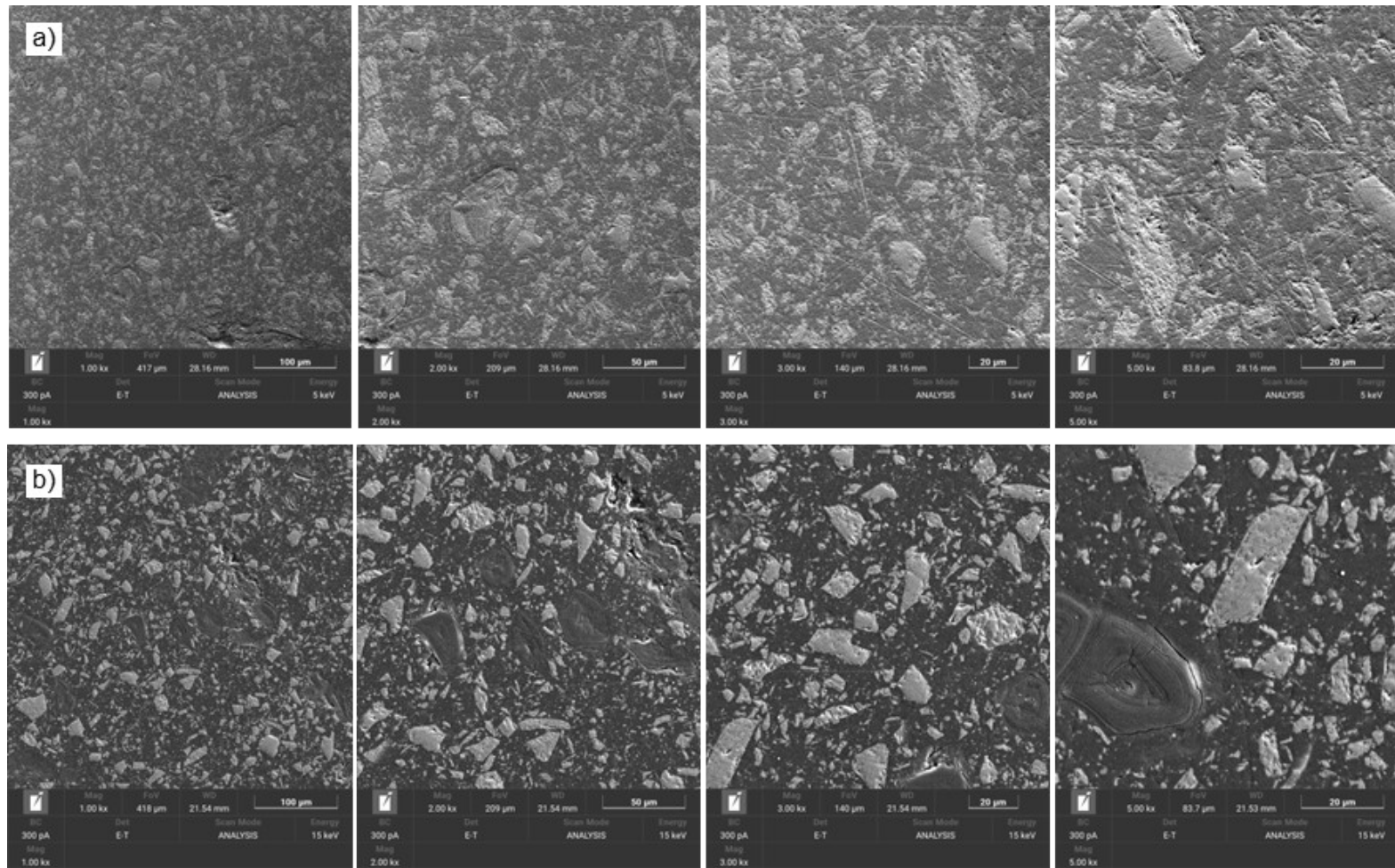


Figure S50. SEM micrographs showing the microstructure of the composites containing: a) OS@AEAPTMS; and b) OS@APTMS.

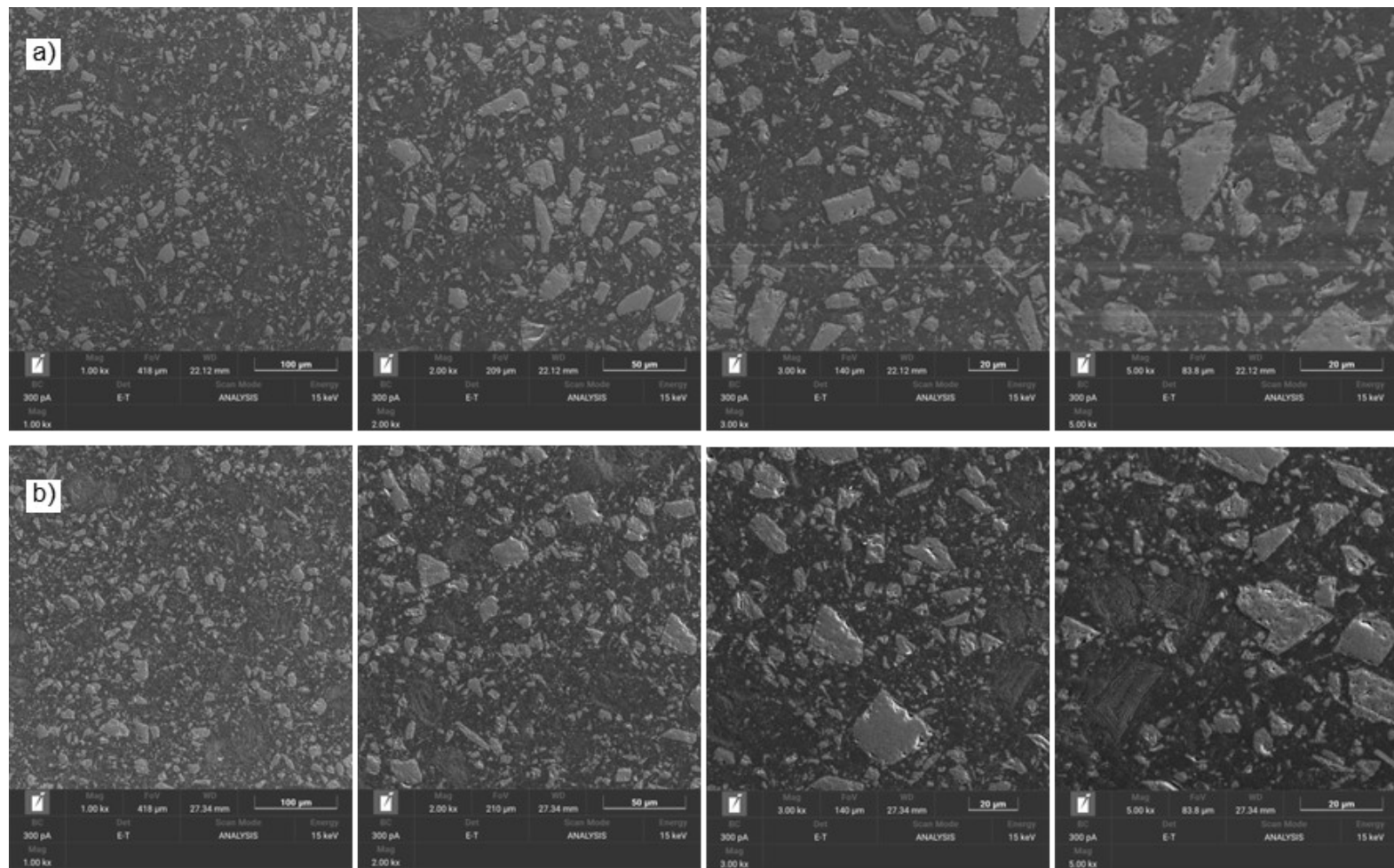


Figure S51. SEM micrographs showing the microstructure of the composites containing: a) OS@MEMO; and b) OS@ODTMS.

10. Static contact angle measurements

Table S9. Analysis of roughness, contact angles, surface interaction force components, cohesion energy, free energy, and critical energy of the resulting composites containing feldspar, native OS and OS@Silanized.

Material	$R_a, \mu\text{m}$	Contact angles, °			Interaction components and surface properties, mJ/m ²							
		θ_W	θ_F	θ_D	γ_s^{LW}	γ_s^+	γ_s^-	γ_s^{AB}	ΔG_{coh}	γ_s	τ_0	γ_c
Feldspar	0.9±0.5	117±7	95±2	51±3	33	3	0.03	0.6	-70	34	-33	33
OS	0.9±0.3	80±2	63±6	52±7	33	0.1	8	2	-45	35	12	33
OS@APTMS	1.0±0.6	118±3	99±3	55±2	31	3	0.2	1	-63	33	-34	31
OS@AEAPTMS	0.6±0.3	97±2	81±6	45±9	37	1	3	4	-54	41	-9	37
OS@MEMO	1.0±0.4	111±5	95±6	48±7	35	4	1	4	-52	40	-26	35
OS@ODTMS	2.2±0.6	109±5	109±1	54±9	32	10	8	18	-18	51	-24	32

(R_a) Roughness; (θ_W) contact angle between the surface and the polar solvent 1 (water); (θ_F) contact angle between the surface and polar solvent 2 (formamide); (θ_D) contact angle between the surface and the apolar solvent (diiodomethane); (γ_s^{LW}) the interaction component related to the Lifshitz-van der Waals forces; (γ_s^+) the electron-accepting component; (γ_s^-) the electron-donating component; (γ_s^{AB}) the acid-base component; (ΔG_{coh}) the free energy variation; (τ_0) the water adhesion tension; (γ_s) the surface free energy; and (γ_c) the critical surface energy. Results are presented as the average ± SD (n = 3).

Table S10. Analysis of contact angle of the biofillers. Surfaces were prepared by the mild pressing of the corresponding powder to form a flat pellet suitable for the measurements.

	Contact angles, °			Water adsorption time of 5 µL droplet, s
Material	θ_W	θ_F	θ_D	
OS	45 ± 5	a	a	5
OS@APTMS	105 ± 5	43 ± 2	11 ± 4	10-15 ^b
OS@AEAPTMS	84 ± 5	66 ± 5	19 ± 2	3-5 ^c
OS@MEMO	a	a	a	d
OS@ODTMS	107 ± 3	87 ± 5	52 ± 4	e

; (θ_W) contact angle between the surface and the polar solvent 1 (water); (θ_F) contact angle between the surface and polar solvent 2 (formamide); (θ_D) contact angle between the surface and the apolar solvent (diiodomethane); Results are presented as the average ± SD (n = 3).

^a Could not be determined; ^b 10-15 s starts the adsorption, but after 120s the droplet is completely adsorbed; ^c 10-15 s starts the adsorption, but after 30s the droplet is completely adsorbed; ^d The droplet is adsorbed instantaneously; ^e The droplet is not adsorbed.

11. References

- 1 B. Sánchez-Sevilla, M. Olmedo-Navarro, J. M. Pérez, J. A. Martínez-Lao and I. Fernández, *ChemistrySelect*, 2023, **8**, e20230034.
- 2 H. Yang, R. Yan, H. Chen, D. H. Lee and C. Zheng, *Fuel*, 2007, **86**, 1781–1788.
- 3 R. J. Hunter, R. H. Ottewill and R. L. Rowell, *Zeta Potential in Colloid Science: Principles and Applications*, Elsevier Science, 2013.
- 4 J. F. Miller, K. Schätzel and B. Vincent, *Journal of Colloid and Interface Science*, 1991, **143**, 532–554.